nature communications

Article

https://doi.org/10.1038/s41467-024-51169-0

A lactobacilli-based inhaled live biotherapeutic product attenuates pulmonary neutrophilic inflammation

Received: 16 April 2024

Accepted: 31 July 2024

Published online: 19 August 2024

Check for updates

Teodora Nicola[1,7], Nancy Wenger[1,7], Xin Xu[2,3], Michael Evans[1], Luhua Qiao[1], Gabriel Rezonzew[1], Youfeng Yang[1], Tamas Jilling[1], Camilla Margaroli[2,3,4], Kristopher Genschmer[2,3], Kent Willis[1], Namasivayam Ambalavanan[1], J. Edwin Blalock[2,3], Amit Gaggar[2,3,5,8] & Charitharth Vivek Lal[1,3,6,8]

Bronchopulmonary dysplasia (BPD) is a chronic lung disease of prematurity. Exposure to noxious stimuli such as hyperoxia, volutrauma, and infection in infancy can have long-reaching impacts on lung health and predispose towards the development of conditions such as chronic obstructive pulmonary disease (COPD) in adulthood. BPD and COPD are both marked by lung tissue degradation, neutrophil influx, and decreased lung function. Both diseases also express a change in microbial signature characterized by firmicute depletion. However, the relationship between pulmonary bacteria and the mechanisms of downstream disease development has yet to be elucidated. We hypothesized that murine models of BPD would show heightened acetylated proline-glycine-proline (Ac-PGP) pathway and neutrophil activity, and through gain- and loss-of-function studies we show that Ac-PGP plays a critical role in driving BPD development. We further test a inhaled live biotherapeutic (LBP) using active *Lactobacillus* strains in in vitro and in vivo models of BPD and COPD. The *Lactobacillus*-based LBP is effective in improving lung structure and function, mitigating neutrophil influx, and reducing a broad swath of pro-inflammatory markers in these models of chronic pulmonary disease via the MMP-9/PGP (matrix metalloproteinase/proline-glycine-proline) pathway. Inhaled LBPs show promise in addressing common pathways of disease progression that in the future can be targeted in a variety of chronic lung diseases.

Bronchopulmonary dysplasia (BPD) is a chronic lung disease of very premature infants characterized by lung inflammation and dysregulation of alveolar and vascular development and is associated with long-term respiratory sequelae[1–3]. Chronic obstructive pulmonary disease (COPD) in older adults is a major contributor to respiratory morbidity, and its development can be linked to early life exposure to maternal cigarette smoke, respiratory illness, and premature birth[4,5]. Both diseases are characterized by neutrophilic lung inflammation and marked by increased protease activity and increased gamma-proteobacteria signature[6–10]. The lungs are not sterile and harbor a

[1]Division of Neonatology, Department of Pediatrics, University of Alabama at Birmingham, Birmingham, AL, USA. [2]Division of Pulmonary, Allergy and Critical Care Medicine, Program in Protease and Matrix Biology, University of Alabama at Birmingham, Birmingham, AL, USA. [3]Lung Health Center, University of Alabama at Birmingham, Birmingham, AL, USA. [4]Division of Molecular and Cellular Pathology, Department of Pathology, University of Alabama at Birmingham, Birmingham, AL, USA. [5]Birmingham VA Medical Center, Birmingham, AL, USA. [6]Marnix Heersink Institute of Biomedical Innovation, University of Alabama at Birmingham, Birmingham, AL, USA. [7]These authors contributed equally: Teodora Nicola, Nancy Wenger. [8]These authors jointly supervised this work: Amit Gaggar, Charitharth Vivek Lal. e-mail: clal@uabmc.edu

low biomass microbiota[11], although the mechanisms by which these bacteria contribute to this inflammation have not yet been determined. We previously identified that infants with severe BPD had decreased firmicutes, specifically *Lactobacilli*, in their lungs with a corresponding increase in markers of neutrophilic inflammation[12].

Here we show that a live biotherapeutic product (LBP) containing a blend of natural commensal *Lactobacillus* strains greatly reduces neutrophilic inflammation in models of chronic lung diseases BPD and COPD. These findings are further tested in gain-of-function and loss-of-function models in vitro, gnotobiotic murine models, and humanized in vivo models of lung diseases[13,14]. We then formulate a *Lactobacillus* LBP that is commercially engineered by spray drying to imbue particle characteristics amenable for effective inhaled delivery into the distal regions of the lung. We demonstrate that the inhaled *Lactobacillus* LBP is effective in reducing neutrophilic inflammation and improving lung structure through the MMP-9/PGP (matrix metalloproteinase/proline-glycine-proline) matrikine[15] pathway in mouse models of BPD and COPD. Further, we identify L(+) lactic acid as an active component of these bacteria that induces an anti-inflammatory effect. These results provide both (1) a discrete proteolytic mechanism by which the lung bacteria enhance neutrophilic inflammation and subsequent local tissue injury and (2) a potential avenue for commensal *Lactobacilli*-based inhaled LBPs as a therapeutic approach for chronic lung disease.

Results

Airways of premature infants with severe BPD are marked by decreased Lactobacilli, increased neutrophilic inflammation, and increased matrikine levels

We discovered infants with severe BPD have decreased *Lactobacilli*, increased proteobacteria, and increased proteobacteria endotoxin concentrations in their airways (Fig. 1A)[12]. In order to further understand the potential link between bacteria and tissue destruction, matrikines Ac-PGP and MMP-9 were analyzed. The TA from infants with severe BPD had higher Ac-PGP and MMP-9 concentrations when compared to controls (Fig. 1B, C). In addition, markers of neutrophil activity, including myeloperoxidase (MPO) and neutrophil elastase (NE) were increased in TA from infants with severe BPD as compared to controls, indicating a significant neutrophil influx (Fig. 1D, E).

Double-hit mouse model of severe BPD shows significant alveolar hypoplasia and matrikine surge

To define the role of airway bacteria in BPD pathogenesis, we utilized the established LPS and hyperoxia double-hit murine BPD model[16]. Mouse pups exposed to both LPS and hyperoxia exhibited severe alveolar hypoplasia (Fig. 1F) with worsened radial alveolar counts (RAC) (Fig. 1G) and worse pulmonary functions (Fig. 1H, I) when compared with control animals in hyperoxic and normoxic conditions. LPS-exposed animals showed an increase in Ac-PGP concentrations compared to controls in normoxia (Fig. 1J). MPO levels followed the same pattern, rising with LPS exposure alone and when combined with hyperoxia (Fig. 1K).

Gain-of-function of matrikine Ac-PGP produces severe BPD, loss-of-function protects in mice

To elucidate the causative role of Ac-PGP in the pathogenesis of BPD, newborn mice were dosed with exogenous Ac-PGP and exposed to normoxia or hyperoxia. Mice exposed to Ac-PGP alone showed severe lung hypoplasia (Fig. 2A) and significantly reduced RAC when compared to controls (Fig. 2B). Both control and Ac-PGP mice showed decreased RAC when exposed to hyperoxia, with Ac-PGP + hyperoxia-exposed mice showing further reduction in RAC compared to hyperoxia controls. Additionally, MPO in the lungs increased in mice exposed to Ac-PGP in both normoxia and hyperoxia compared to controls (Fig. 2C). The control mice in hyperoxia showed increased MPO when compared to the normoxia control mice, while the Ac-PGP-exposed mice had higher MPO in hyperoxia. In order to assess the effect of Ac-PGP on pulmonary circulation, echocardiograms were performed on the studied animals. In both the normoxia and hyperoxia exposure groups, Ac-PGP exposure resulted in right ventricular hypertrophy (RVH) when compared with control animals (Fig. 2D).

We hypothesized that loss of Ac-PGP function would protect against the development of a BPD phenotype. In this case, mice were treated with the Ac-PGP antagonist arginine-threonine-arginine (RTR) during concomitant LPS and hyperoxia exposure. We noted that the hyperoxia-exposed mice dosed with LPS and RTR had significantly higher alveolar counts when compared to LPS and hyperoxia-exposed mice (Fig. 2E). In hyperoxia, mice treated with RTR showed lower concentrations of MPO than mice exposed to LPS alone (Fig. 2F) and had less severe RVH (Fig. 2G).

These findings suggest the causative role of Ac-PGP in BPD and show that treatment with an Ac-PGP antagonist may be protective.

Lactobacillus-based LBP improves lung morphology and function in double-hit murine BPD model

Since our previous study[12] revealed that infants with severe BPD have a decrease in airway *Lactobacillus* abundance, we treated double-hit BPD injury mice (hyperoxia + *E. coli*) with the *Lactobacillus* LBP.

Mouse pups were dosed intratracheally with the LBP in order to determine if treatment directly to the lungs would counteract the lung injury typically observed in this model. Lung morphology analysis revealed that injured mice had higher RAC when treated with the LBP, which suggests less alveolar hypoplasia and simplification (Fig. 2H, I). When mice exposed to hyperoxia and *E. coli* were treated with LBP, the concentration of MMP-9 in lung tissue and MMP-9, NE, and MPO protein in BAL decreased, suggesting a lower neutrophilic influx (Fig. 2J–L and Supplementary Fig. 1). IL-6 and CRP protein levels also decreased in the double injury mice treated with LBP (Fig. 2M, N). Biomarkers in mice dosed with the LBP alone in air did not increase pro-inflammatory protein levels and in hyperoxia reduced MMP-9 mRNA and protein, NE, and CRP protein (Supplementary Fig. 2). These results highlight the impact of attenuating neutrophilic inflammation and associated tissue damage through the use of a *Lactobacillus*-based LBP.

Live *Lactobacillus* strain blend reduces MMP-9 levels more than individual strains

Prior to testing the LBP in the BPD model, we explored combinations of *Lactobacilli* to find an optimal anti-neutrophilic formulation. We exposed human bronchial epithelial cells (HBEC) to *E. coli* to generate an in vitro model of lung epithelial inflammation. Cells were treated with seven individual *Lactobacillus* strains: *L. casei, L. paracasei, L. reuteri, L. fermentum, L. plantarum, L. acidophilus*, and *L. rhamnosus*. *L. plantarum, L. acidophilus*, and *L. rhamnosus* (abbreviated as P, A, and R) performed better than the other four strains in reducing MMP-9 expression compared to the *E. coli* exposure group with no treatment as well as when compared to each other (Fig. 3A). Different ratios of the top-performing strains were tested, and the 1:1:1 ratio of P:A:R reduced MMP-9 expression the most (Fig. 3B). Therefore, these three strains in a 1:1:1 ratio were advanced for use in all future experiments. When *E. coli*-exposed cells were treated with a blend of these strains, MMP-9 expression decreased more than when treated with individual strains (Fig. 3C).

Live bacteria active components reduce MMP-9

In order to identify potential anti-inflammatory agents, we isolated different cellular components and byproducts of the *Lactobacillus* strains. Cell culture supernatant (Fig. 3D) was effective in reducing MMP-9 expression in a dose-dependent manner, as were isolated teichoic acid, peptidoglycan, polysaccharide, and S-layer (Supplementary

https://doi.org/10.1038/s41467-024-51169-0

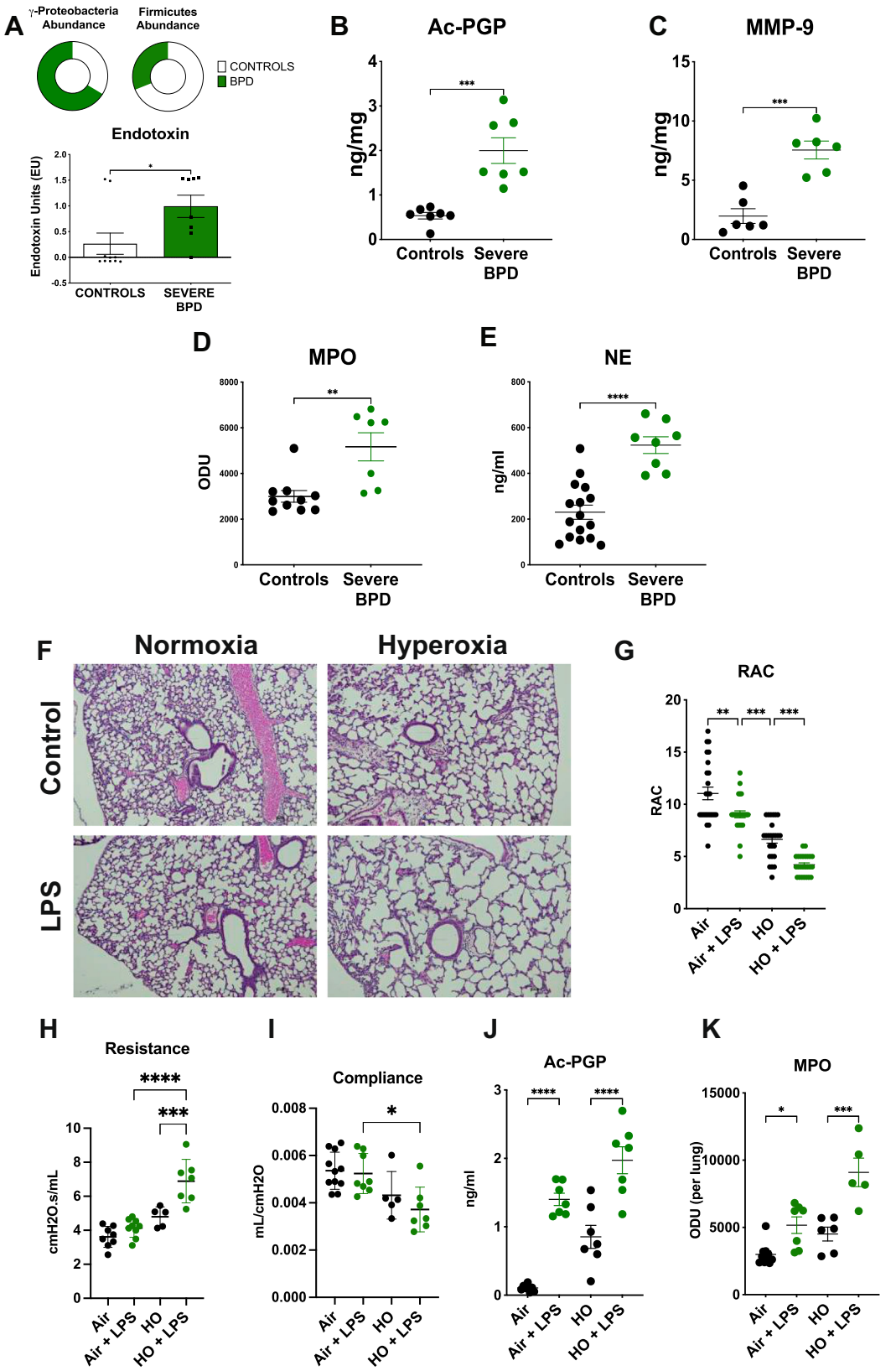

Fig. 3). As *Lactobacilli* are known lactic acid producers, we measured the effect of each strain's supernatant on lactate gene expression in the other strains individually and as blends. Using *L. acidophilus* as a representative example, we found that its supernatant increased lactate gene expression of the other strains individually and combination (Fig. 3E). We then measured L(+) and D(−) lactic acid output of each strain (Fig. 3F). The more abundant L(+) lactic acid was effective at reducing MMP-9 expression in vitro while D(−) was not (Fig. 3G, H).

We then dosed L(+) lactic acid intratracheally to WT mice exposed to intratracheal LPS for 10 days. Analysis of histological images (Fig. 4A) revealed an improvement in mean linear intercept (MLI) upon

Fig. 1 | Severe BPD is marked by decreased *Lactobacilli*, increased proteobacteria, and neutrophil influx mediated by the MMP-9/Ac-PGP pathway. **A** Infants with severe BPD had increased proteobacteria, decreased firmicutes, and increased endotoxin levels compared to controls as measured by 16s microbiome sequencing ($P = 0.0284$) (data from ref. 12). Infants with severe BPD had higher concentrations of **B** Ac-PGP ($P = 0.0003$), **C** MMP-9 ($P = 0.0002$), **D** MPO ($P = 0.0023$; Control $N = 10$, BPD $N = 7$ samples), and **E** NE protein ($P < 0.0001$; Control $N = 16$, BPD $N = 8$ samples) in their tracheal aspirates than controls. Unpaired *t*-test. Ac-PGP was measured by tandem mass spectrometry; MMP-9, MPO, and NE were measured by ELISA. Control $N = 7$, BPD $N = 7$ samples. Mice were exposed to hyperoxia (HO) from PN3- PN14, LPS on PN3, 6, 9, and 12, and euthanized on PN14. **F** Mice exposed to HO + LPS demonstrated severe alveolar hypoplasia and simplification. Tissue slices from harvested lung tissue were photographed at 4x magnification after hematoxylin and eosin (H&E) staining. **G** Radial alveolar count (RAC) decreased in LPS mice. $N = 24$ samples. Pulmonary function worsened as measured by **H** resistance (increased) (Air $N = 7$, Air+LPS $N = 8$, HO $N = 5$, HO + LPS $N = 7$ mice) and **I** compliance (decreased) in HO + LPS mice (Air $N = 10$, Air+LPS $N = 8$, HO $N = 5$, HO + LPS $N = 7$ mice). LPS-exposed mice had higher concentrations of **J** Ac-PGP (Air $N = 8$, other groups $N = 7$ mice) and **K** MPO in the bronchoalveolar lavage fluid (BAL) (Air $N = 10$, Air + LPS $N = 7$, HO $N = 6$, HO + LPS $N = 5$ mice). One-way ANOVA, Tukey's multiple comparisons test. Bars represent the median ± interquartile range. $^{*}P < 0.05$, $^{**}P < 0.01$, $^{***}P < 0.001$, $^{****}P < 0.0001$.

treatment with 1.0 µg/g lactic acid compared to LPS-exposed mice (Fig. 4B). Lactic acid treatment also reduced MMP-9 expression in the lung tissue (Fig. 4C) in comparison to mice who received LPS exposure without treatment. A 3-day model of LPS exposure produced similar biochemical results without significant changes in tissue structure (Supplementary Fig. 4). These findings emphasize the function of a discrete *Lactobacillus* byproduct as a modulator of MMP-9 activity in vitro and in vivo.

In vivo LBP lactic acid production, distribution, and clearance

Having identified L(+) lactic acid as an active anti-inflammatory moiety, we sought to determine the relationship between *Lactobacillus* strain growth and lactic acid production. We first grew each *Lactobacillus* strain in vitro and measured the L(+) lactic acid output of each strain. While *L. acidophilus* maintained a relatively low concentration, it was the highest producer of L(+) lactic acid out of the three strains (Supplementary Fig. 5). We then inoculated healthy WT mice intratracheally with a blend of the three strains to model inhaled distribution and clearance of an LBP. When visualized using fluorescence microscopy, the blend (labeled in green) appeared localized to the lung tissue with the characteristic rod shape of *Lactobacilli* visible in the 40x magnification inset (Fig. 4D). While the cell counts in the lungs steadily decreased over 72 h as measured by whole lung colony counts (Fig. 4E), L(+) lactic acid levels stayed relatively consistent through 72 h (Fig. 4F). Administration of the live bacteria produced a transient inflammatory response with brief increases in MMP-9, CRP, and IL-6 proteins that peaked at 4–8 h and returned to baseline by 16–24 h (Fig. 4G–I).

Table 1 | Aerosol and physical characteristics of three spray-dried powder formulations

	1 – lead	1 – repeat run	2	3
Delivered dose (mg)	26.82	25.6	--	26.32
Delivered dose (% of 30 mg)	88%	85%	--	86%
MMAD (µm)	2.4	2.3	--	2.5
GSD	1.7	--	--	1.6
FPF < 5.0µm	94%	95%	--	94%
FPF < 3.3µm	73%	76%	--	74%
gPSD, 4 bar (µm) D10/D50/D90	0.487/ 1.40/3.02	--	0.602/ 1.35/2.74	0.459/ 1.38/3.00
DSC Tg (Tg1/Tg2)	40.8 C/ 124.7 C	--	43.1 C/ 121.3 C	39.6 C/ No data
Bulk density (g/cc)	0.26	--	0.28	0.19
Water activity	0.082	--	0.079	0.094
Moisture (KF)	1.48%	1.48%	1.38%	1.46%
Viability (CFU/g)	3.8×10^9	4.6×10^9	--	1.7×10^9

MMAD median mass aerodynamic diameter, *GSD* geometric size distribution, *FPF* fine particle fraction, *gPSD* geometric particle size, *DSC* differential scanning colorimetry, *Tg* glass transition temperature, *KF* Karl Fischer, *CFU* colony forming units.

Engineered LBP particles show favorable delivery and viability characteristics

Using the three live *Lactobacillus* strains, we engineered an inhalable particle containing live bacteria, spray-dried with stabilizers and excipients (trehalose, leucine, sodium citrate, polysorbate) to elicit favorable characteristics for deep lung delivery. Several rounds of spray drying optimization (Table 1) yielded a lead formulation, as shown in scanning electron microscope images (Fig. 5). The formulation had a small median mass aerodynamic diameter (MMAD) of 2.4 µm as measured by gravimetric impaction (Table 1). About 74% of the total powder mass was <3.3 µm, meaning that ~74% of the particles were small enough to be delivered to the distal lung. About 99% viability of the strains was retained by comparing cell plate counts pre- and post-drying. These tests validated that a live bacteria blend could be successfully engineered with favorable particle characteristics for deep lung delivery while maintaining excellent viability.

LBP blend antibiotic susceptibility and resistance panel

The antibiotic susceptibility and resistance profile of each *Lactobacilli* strain was assessed in order to identify potential rescue medications, ensuring safety in a therapeutic setting. Each strain was plated individually with 51 FDA-approved antibiotics and the minimum inhibitory concentration (MIC) was determined (Supplementary Table 1). On a per-strain basis, the LBP was susceptible to 34 and resistant to 17 of the antibiotics. When plated and incubated with the antibiotic as a blend, the LBP was resistant to ceftazidime TX 256, gentamicin, and the CT variant of ESBL CT/CL, although the strains incubated individually were susceptible (Supplementary Table 2).

Inhaled *Lactobacillus* LBP attenuates lung tissue damage and inflammation in murine models of COPD

Having generated a flowable powder for inhalation containing viable bacteria with anti-inflammatory properties, we proceeded to test the *Lactobacillus* LBP in preclinical animal models of COPD. Based on the promising results with the LBP in the BPD double-hit mouse model as well as mechanistic commonalities between the two diseases, we evaluated the anti-inflammatory activity of the LBP in three different mouse models of COPD.

First was an etiological COPD model using cigarette smoke. After 4 weeks of smoking, mice showed minimal lung tissue damage compared to mice who received air (Fig. 6A, B). However, smoke exposure did heighten MMP-9 mRNA expression in lung tissue and MMP-9 protein in the serum (Fig. 6C, D). Treatment IT with the *Lacto* LBP led to a decrease in MMP-9 mRNA in lung tissue and protein in serum (Fig. 6C, D). When treated with the LBP, mice also showed an increase in protective IgA protein in the BAL compared to controls (Fig. 6E).

Next, we tested both structural injury and inflammation in COPD. We first conducted a dose tolerability test to assess how much LBP powder mice could tolerate (Supplementary Table 3). Eight 10–12-week-old C57BL6 mice were used per group. Mice were dosed with either a PBS control, 5 mg of placebo, 5 mg of LBP in a single dose, or 2.5 mg of LBP followed by another 2.5 mg an hour later every other day

https://doi.org/10.1038/s41467-024-51169-0

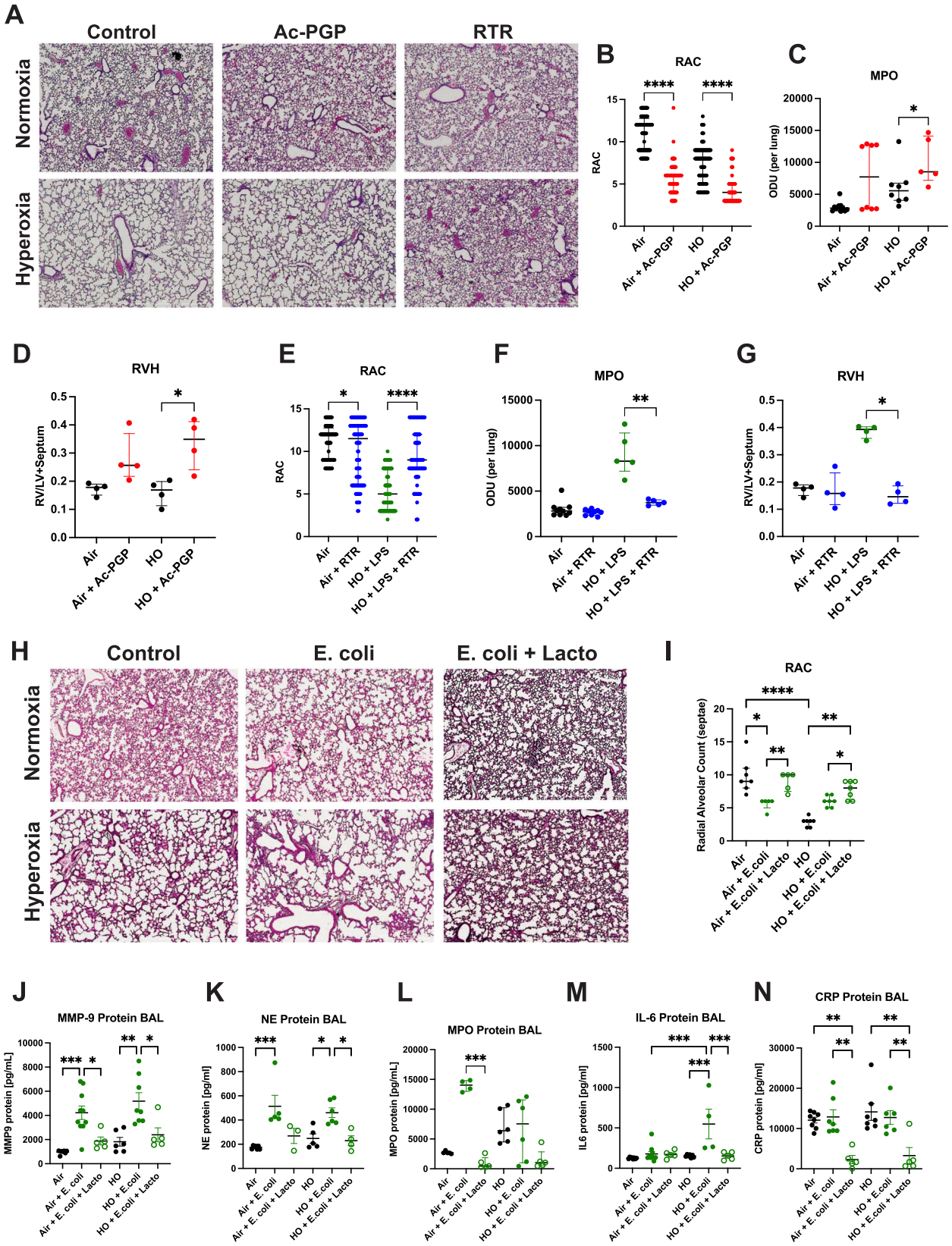

for 1 week. Mice were sacrificed 24 h after their last dose. Mice tolerated both doses of 5 mg of LBP with no deaths (Supplementary Fig. 6A). Body weight (Supplementary Fig. 6B) and temperature (Supplementary Fig. 6C) remained within clinically normal ranges by the final day of dosing. Five vital sign parameters were measured by MouseOximeter Plus (Starr Life Sciences). Improved oxygen saturation (Supplementary Fig. 6D) was observed in the LBP-treated mice compared to PBS control and placebo. All other vital signs showed no significant changes (Supplementary Fig. 6E–H). Furthermore, the lungs, serum, kidney, and liver PCR for bacterial DNA showed that the tissues were free of the *Lactobacilli* strains specific to the LBP blend (Supplementary Fig. 7). To ensure the animals tolerated longer dosing

Fig. 2 | Ac-PGP drives tissue damage and *Lacto* LBP reduces neutrophilic inflammation. Ac-PGP and LPS exposure each in combination with hyperoxia (HO) resulted in severe alveolar hypoplasia and simplification. **A** Treatment with RTR (arginine-threonine-arginine) improved alveolar structure. H&E staining, 4x magnification. **B** RAC decreased upon dosing with Ac-PGP or LPS ($N = 120$ samples) and **C** MPO expression increased in Ac-PGP exposure in HO ($P = 0.0451$; Air $N = 11$, Air +Ac-PGP $N = 8$, HO $N = 8$, HO+Ac-PGP $N = 5$ mice). **D** Right ventricular hypertrophy (RVH) increased in Ac-PGP + HO mice. ($P = 0.028$; $N = 4$ mice). **E** RAC improved upon treatment with RTR. $N = 120$ samples. **F** MPO expression increased upon exposure to LPS + HO and reduced upon RTR treatment ($P = 0.0079$; Air $N = 10$, Air + RTR $N = 9$, HO $N = 5$, HO + LPS + RTR $N = 5$ mice). **G** RVH decreased in LPS + HO mice treated with RTR ($P = 0.0187$; $N = 4$ mice). Mann–Whitney *U*-test, Kruskal–Wallis, Dunn's multiple comparisons test. **H** Hyperoxia exacerbated alveolar simplification in mice exposed to *E. coli* intranasally, while intratracheal LBP treatment improved tissue structure in *E. coli* + HO mice. H&E staining, 4x magnification. **I** RAC decreased in HO + *E. coli* exposure and restored to normal with LBP treatment. Air $N = 7$, Air + *E. coli* $N = 5$, Air + *E. coli* + Lacto $N = 5$, HO groups $N = 5$ mice each. **J** BAL MMP-9, **K** NE, **L** MPO, **M** IL-6, and **N** CRP decreased upon treatment with LBP. One-way ANOVA, Tukey's multiple comparisons test. Air $N = 7$, Air + *E. coli* $N = 10$, Air + *E. coli* + Lacto $N = 5$, HO $N = 6$, HO + *E. coli* $N = 8$, HO + *E. coli* + Lacto $N = 5$ mice. Bars represent the median ± interquartile range. $^{*}P < 0.05$, $^{**}P < 0.01$, $^{***}P < 0.001$, $^{****}P < 0.0001$.

durations, a 1.5 mg dose of LBP administered every other day was selected for future studies.

In parallel 3-week experiments, mice were exposed to either PPE or PPE + LPS and treated concurrently with the LBP. PPE generated emphysema in mice, while the LPS added a measure of bacteria-induced inflammation to the PPE-driven proteolytic degradation and tissue remodeling (Fig. 6F). As such, mice exposed to both PPE and LPS had emphysema with additional inflammation in the lung tissue (Fig. 6F). Treatment with the LBP improved lung structure compared to both injury groups as measured by reduced MLI (Fig. 6G). Lung mechanics worsened as measured by increased resistance upon exposure to PPE and improved upon treatment with the LBP (Fig. 6H). There was no significant change in compliance (Fig. 6I).

Lung tissue MMP-9 expression increased upon exposure to PPE + LPS and decreased upon treatment with the LBP (Fig. 6J). LBP treatment also resulted in lower MMP-9, NE, CRP, and IL-8 protein in the BAL of PPE + LPS dosing groups, and lower IL-8 in the PPE group (Fig. 6K–N). Protective IgA protein in the BAL increased in every group treated with the LBP (Fig. 6O). LBP treatment resulted in lower MMP-9, NE, and CRP protein in serum (Supplementary Fig. 8). LBP treatment consistently produced lower levels of pro-inflammatory proteins in the lungs and in circulation.

Lactobacillus LBP performs as well as steroids in the post-injury treatment model of COPD

After showing improvement in inflammatory biomarkers and tissue structure given LBP treatment concurrent to injury, we treated mice after injury was established. Mice were exposed to PPE or PPE + LPS and treated with either the LBP or the steroid fluticasone furoate to the lungs. Even when treating mice after injury was established, LBP treatment resulted in significant improvements to lung tissue structure (Fig. 7A, B). Steroid treatment resulted in modest structural improvements consistent with typical mouse healing rates in a 3-week PPE model. The LBP exhibited impressive steroid-like anti-neutrophilic inflammatory action and worked better than and as well as, respectively, the steroid in reducing MMP-9 and CRP protein in BAL (Fig. 7C, D). In fact, the LBP performed better than the steroid in increasing levels of a variety of additional pro-inflammatory proteins in the BAL, including MIP-3b, IL-11, IL-16, and TIMP1 (Supplementary Fig. 9).

Lactobacillus LBP shows favorable safety and biodistribution profile in COPD mouse model

To characterize the inhaled LBP's safety profile, we tested the drug product in a respiratory safety and biodistribution study using PPE model mice. Mice were exposed to PPE or a PBS control as previously described and then treated daily for 14 days with nothing, placebo powder, 1 mg LBP, or 3 mg LBP. On Day 21, half the mice had their vitals taken and were designated as the terminal sacrifice cohort. On Day 28, the second half of the mice had their vitals taken and were designated as the recovery sacrifice cohort. All mice in both the terminal and recovery sacrifice groups survived the daily dosing (Fig. 8A). In both terminal and recovery groups, vital signs did not indicate adverse responses to LBP powder inhalation (Fig. 8B–O). Despite some variation between groups, values did not exceed normal ranges.

At terminal and recovery sacrifice time points, lung, brain, heart, liver, kidneys, spleen, and serum were harvested. Bacterial gDNA was extracted from each tissue and PCR was run using primers specific to each *Lactobacillus* strain in the LBP (P, A, and R) to see if bacteria distributed beyond the target tissue of the lungs. PCR gels confirmed that no *Lactobacillus* LBP remained in the lungs at the time of terminal sacrifice or recovery sacrifice, nor did it travel to distal tissues (Fig. 8P, Q).

Identifying additional pathways of interest affected by *Lactobacillus* LBP

To investigate further what pathways are at play upon LBP treatment in multiple injury models, we conducted RNA sequencing. HBE cells were exposed to *Pseudomonas aeruginosa*, cigarette smoke, or smoke + *Pseudomonas* and treated with the LBP or a PBS control. Across the three sets of exposures, treatment with the LBP caused the up- or down-regulation of 48 genes (Supplementary Fig. 10B). A heat map of the gene expression patterns revealed similar changes in expression across the *Pseudomonas* and *Pseudomonas* + smoke injury groups, while smoke exposure alone did not elicit a strong response (Supplementary Fig. 10C). Treatment with the LBP produced a near inverse expression profile, downregulating genes upregulated by injury and vice versa. Four canonical pathways were affected by the LBP in the same way in all three injury models: cellular response to heat stress, chaperone-mediated autophagy, the role of PKR in interferon induction and antiviral response, HF1α signaling (Supplementary Fig. 10D). We also examined a key pathway of interest, the NF-kB pathway. Common genes included heat shock proteins (HSP) and CXC motif chemokine ligands and receptors (CXCL, CXCR) (Supplementary Fig. 10E).

Discussion

Our study mechanistically determines the impact of *Lactobacilli* in the reduction of neutrophilic inflammation in chronic lung diseases such as BPD and COPD (Fig. 9). Specifically, the identification of bacteria as critical to regulating lung protease activity linked to matrikine generation, extracellular matrix (ECM) turnover, and chronic neutrophilic inflammation provides a paradigm for the progression of structural lung disease. In our in vivo experiments, LPS exposure resulted in elevated markers of neutrophilic inflammation and evidence of reduced alveolarization consistent with the presentation of BPD[1]. This was seen independent of hyperoxia exposure, although hyperoxia appeared to potentiate the effects. This is consistent with previous human studies showing that infants with severe BPD have an airway microbial signature that is defined by decreased *Lactobacillus* abundance and that smokers who develop COPD have lower airway dysbiosis and inflammation-driven injury[2,12,17,18].

Ac-PGP generation appears to be important and causative in the development of BPD and COPD. This discovery was made through the generation of Ac-PGP gain and loss of function murine models. Through intranasal instillation of Ac-PGP, markers of neutrophilic

https://doi.org/10.1038/s41467-024-51169-0

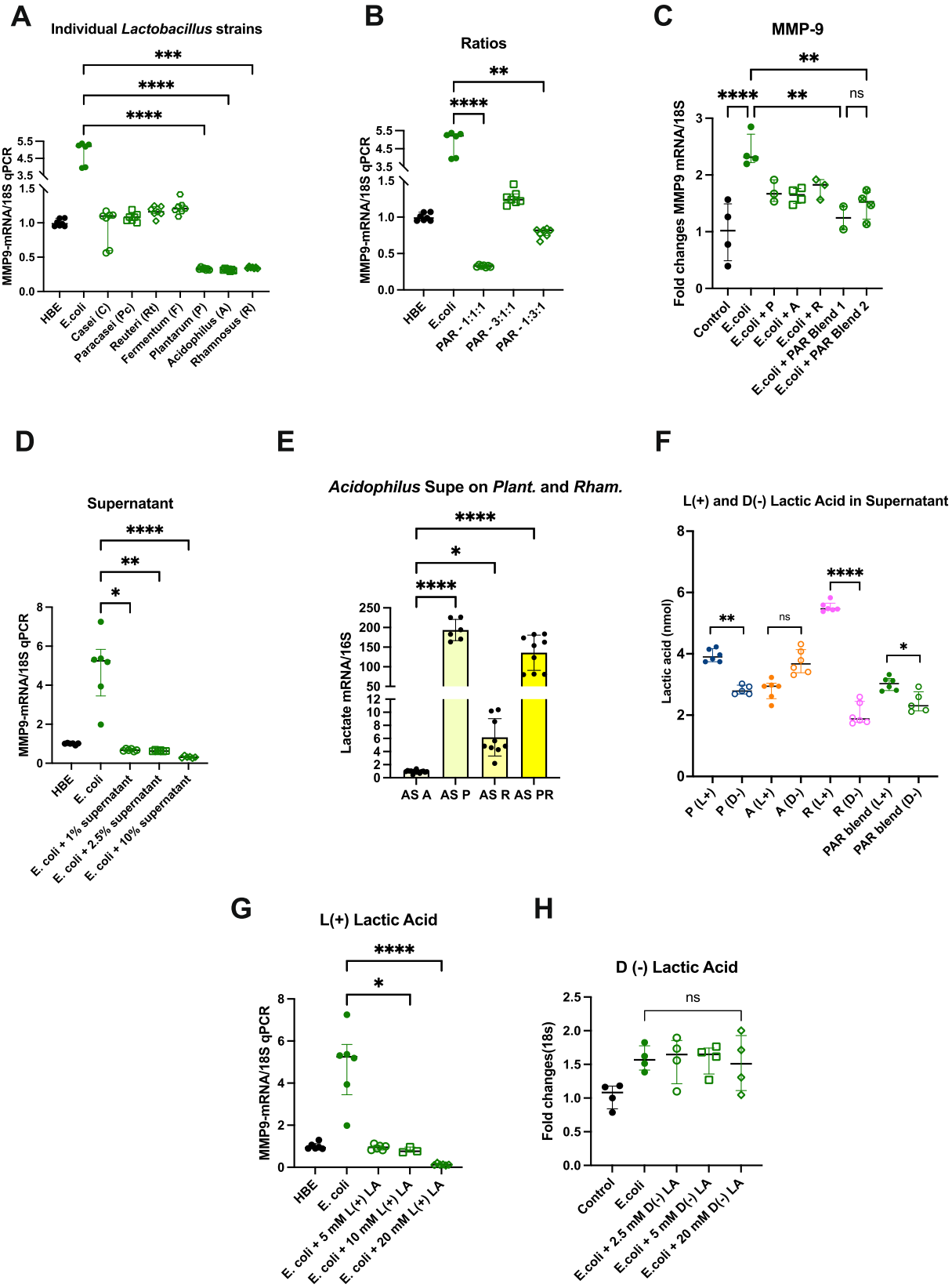

inflammation (MPO) increased independently of hyperoxia. Worsening alveolar simplification (decreased RAC) and abnormal vascular development (increased RVH) were also noted. In mice treated with RTR, markers of neutrophilic inflammation decreased. They also showed an increase in the number of alveoli and a decrease in RVH, suggesting improved alveolar and vascular development. RTR binds and neutralizes PGP sequences and has been noted to attenuate lung damage in murine models of acute lung injury/acute respiratory distress syndrome and allergic airway disease[19,20].

Based on the importance of the presence or absence of *Lactobacillus* in the lung microenvironment, we examined multiple *Lactobacillus* strains for their anti-inflammatory activity. The three live strains

Fig. 3 | *Lactobacillus* blend reduces neutrophilic inflammation through L (+) lactic acid production. A Individual strains *L. plantarum* (P), *L. acidophilus* (A), and *L. rhamnosus* (R) reduce MMP-9 expression more than individual strains *L. casei, L. paracasei, L. reuteri*, and *L. fermentum* compared to *E. coli* exposure alone with no *Lactobacillus* treatment and compared to each other. $N = 7$. **B** Different ratios of blended P, A, and R reduce MMP-9 to varying degrees. $N = 7$ wells. **C** A blend of P, A, and R performed better than individual strains in reducing MMP-9 in human bronchial epithelial (HBE) in vitro model of noxious stimuli exposure. $N = 4$ wells. **D** *Lactobacillus* blend culture supernatant in increasing concentrations reduces MMP-9 expression. $N = 6$. **E** Individual live *Lactobacillus* strains were transfected with supernatant from the other three strains in the blend. *L. acidophilus* supernatant cultured with live A, P, R, and PR blend increased lactate gene expression of P and the PR blend (shown as a representative example). AS A $N = 13$, AS P $N = 6$, AS R $N = 9$, AS PR $N = 9$ wells. **F** *Lactobacillus* strains produce more L (+) lactic acid than D (+) lactic acid individually and as a blend. $N = 6$ wells. **G** L (+) lactic acid reduces MMP-9 expression in HBE cells exposed to *E. coli* ($N = 6$ wells), while **H** D (−) lactic acid does not ($N = 4$ wells). Kruskal–Wallis test, Dunn's multiple comparisons. Cell culture performed in triplicate. Bars represent the median ± interquartile range. $^{*}P < 0.05$, $^{**}P < 0.01$, $^{***}P < 0.001$, $^{****}P < 0.0001$.

L. plantarum, L. acidophilus, and *L. rhamnosus* (P, A, R) performed better in synergy rather than alone in reducing MMP-9 in in vitro models. We found that bacterial supernatant isolated from the blend of *Lactobacillus* strains was effective in reducing MMP-9 at a similar magnitude as live bacteria. There are a variety of bacterial components with anti-inflammatory capacity; for example, exosomal microRNA is a source of anti-inflammatory action[16] that would be present in bacterial supernatants. We observed crosstalk between strains, as isolated supernatant from one strain had a direct impact on the lactate gene expression of the other strains.

A key finding was a reduction in MMP-9 in vitro by L(+) lactic acid, which *Lactobacilli* naturally produce, emphasizing an important role for L(+) lactic acid as an anti-inflammatory molecule and marker of bacterial activity. While in vivo the lungs cleared the bacteria over time, this active metabolite remained. Mice treated with L(+) lactic acid IT showed modest improvements in lung structure and MMP-9, supporting the in vitro results. However, dosing was limited as mice could only tolerate low doses before showing respiratory irritation. When inhaled, live bacteria act as an efficient delivery mechanism for the multiple anti-inflammatory moieties that they produce. Live bacteria provide an ongoing, sustained release of L(+) lactic acid locally in a more controlled and well-tolerated manner than administering a bolus of LA. Future drug development efforts may focus on a sustained release L(+) lactic acid-based drug.

A major technological advancement was our creation of the inhaled LBP by particle engineering. By including stabilizers and excipients in the liquid feedstock to protect the bacteria from the pressure and shear forces of the drying process, we successfully maintained a high CFU count after drying. Furthermore, we achieved a small, dense, flowable particle with a higher delivered dose than typical dry powders.

In order to explore the efficacy of a *Lactobacillus*-based therapeutic, we treated the double-hit murine BPD model with the LBP. Partial protection of lung structure and markers of neutrophilic inflammation (MPO, MMP-9, NE) were noted after LBP treatment. These results suggest that supplementing commensal strains to the lung microenvironment may attenuate neutrophilic inflammation and reduce tissue damage associated with the development of BPD.

Across COPD mouse models (smoke, PPE, PPE + LPS), improvements in both pro- and anti-inflammatory biomarkers in the BAL suggest that inhalation of the *Lactobacillus*-based blend successfully reduced inflammation in the lung microenvironment, whether treated concurrently or post-injury. The LBP exerted an anti-inflammatory effect that decreased known pro-inflammatory markers MMP-9, NE, CRP, and IL-8 while elevating anti-inflammatory marker IgA. Similar trends were also observed in the serum, suggesting that the anti-inflammatory action of the LBP in the lungs can trigger signaling cascades at a systemic level.

Transcriptomic data contextualizes the animal biomarker improvements into a broader network of pathways in which LBP has a therapeutic effect. The data confirmed an effect on neutrophil recruitment and activity, as neutrophil ligands CXCL1, 5, and 10 were consistently downregulated by LBP treatment, although the different injury models induced their expression to varying degrees. These CXCL chemokines are implicated in COPD pathogenesis through their interaction with CXC receptors. CXCL1 acts on CXCR2 to recruit neutrophils[21], and CXCL5 is associated with neutrophilia in severe COPD exacerbations[22,23]. MMP-9 breaks down ECM to liberate PGP, which due to its sequence homology with CXC ligands, activates CXCR2[24]. CXCL10 is a CXCR3 ligand involved in immunomodulation; it activates T cells and is highly expressed in the small airway tissue of COPD patients[25,26]. The activity of NF-kB-associated genes was broadly downregulated in the LBP treatment groups, including several CXCLs. There was also a notable decrease in IL-32, an interleukin localized to the alveolar epithelium, and correlated with airway obstruction in smokers with COPD[27]. Although its effects are multifactorial, lactate may play a role in suppressing LPS-induced NF-kB pathway activity and modulating immune cell metabolism[28,29].

An interesting finding was the favorable performance of the LBP compared to fluticasone furoate, a widely studied[30] FDA-approved inhaled corticosteroid found in COPD combination therapies. The LBP reduced MMP-9 and other pro-inflammatory cytokines as well as, and in some cases better than, the steroid in the PPE + LPS COPD mouse model. Prolonged use of steroids for COPD exacerbations is associated with side effects, including increased risk of pneumonia, skin thinning, sepsis, and death[31,32]. Neutrophilic inflammation is steroid-resistant, a major therapeutic gap in the COPD therapeutic landscape.

In the future, our LBP may reduce or replace the need for inhaled steroids by virtue of their strong anti-inflammatory action combined with a more tolerable safety profile and additional potential structural benefits. Safety and biodistribution, as studied in the PPE emphysema model, indicated that inhalation of the LBP did not initiate adverse reactions in diseased mice. The *Lactobacilli* did not translocate to distal tissues or accumulate in the lungs, supporting the hypothesis that the bacteria have a localized yet transient presence in the airways. Furthermore, the LBP is susceptible to the antibiotics Cefuroxime, Azithromycin, Amoxicillin-clavulanate, Piperacillin-tazobactam, and Ceftriaxone, all of which are currently used to treat COPD exacerbations and may be used as rescue medication in a clinical setting.

Preclinical animal data is suggestive, and the safety of the potential drug in humans will be tested in a forthcoming clinical trial. Human adult safety data in COPD will help de-risk the pathway to approval for use of the drug in BPD infants. The development of an inhaled LBP will afford us the opportunity to test the drug for efficacy in patients with long-standing respiratory dysbiosis in a severe disease state. Pulmonary space, unlike the gut, clears bacteria much more effectively and consistently. Therefore, while our data do not suggest that the LBP will make long-term alterations in the microbiome composition, it will allow for the effective delivery of an anti-inflammatory therapeutic effect.

The pathogenesis of chronic lung diseases is complex and multifactorial in nature. We present key mechanistic data linking a proteobacteria-dominant lung microbiome with tissue injury and neutrophilic inflammation in the chronic lung diseases BPD and COPD. An inhaled *Lactobacillus*-based LBP shows promising therapeutic potential, as evidenced by efficacy and safety data in our robust set of BPD and COPD models. Microbial agents as therapeutics are becoming more widely studied to modulate disease, with modalities such as

https://doi.org/10.1038/s41467-024-51169-0

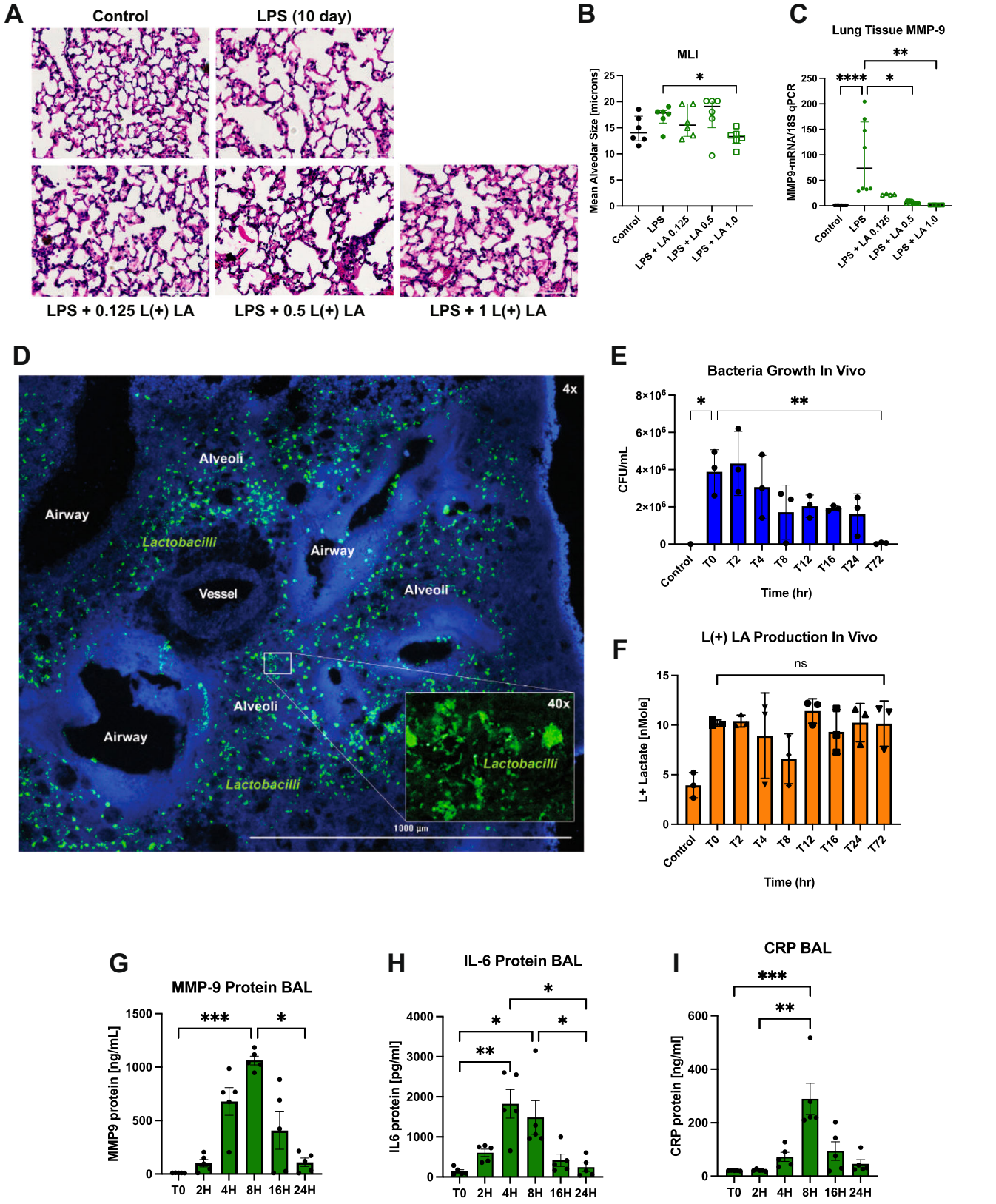

phage therapy gaining traction in treating viral respiratory infections. While symptomatic treatments are available for patients, there remains a lack of preventative or curative chronic therapies for BPD or COPD. Demonstrated performance comparable to an inhaled steroid has major implications in affecting the landscape of standard of care for COPD patients by providing a supplemental or replacement treatment option. These and future studies provide foundational research that may lead to improved care for patients with these chronic and devastating diseases.

Methods

Ethical statement

In a prospective cohort study performed between October 2014 and December 2016, tracheal aspirate (TA) samples were collected at the

Fig. 4 | L (+) lactic acid reduces MMP-9 and is produced by *Lactobacilli* in vivo. Mice exposed to LPS intratracheally for 10 days were dosed with L (+) lactic acid in the lungs. **A** Lung histology images show alveolar simplification upon LPS injury and slight recovery upon LA treatment. H&E staining, 4x magnification. **B** MLI decreased upon treatment with 1 ug/g body weight L (+) LA per mouse ($P = 0.0152$; $N = 6$ mice). **C** Lung tissue MMP-9 expression decreased upon IT L (+) lactic acid treatment (Control $N = 10$, LPS $N = 8$, LA 0.125 $N = 4$, LA 0.5 $N = 12$, LA 1.0 $N = 4$ mice). **D** *Lactobacilli* (green) localizes to the lung epithelium 3 h after intratracheal inoculation to healthy mice. DAPI blue. 4x magnification, 40x magnification on inset. $N = 5$. **E** Healthy mice inoculated with *Lactobacillus* LBP to the lungs show progressive clearance of bacteria via the reduction in colonies over 72 h. **F** Healthy mice inoculated with LBP to the lungs show an increase in L (+) lactic acid production and sustained effect through 72 h post-dose. L(+) LA measured by lactate colorimetric assay. $N = 3$ mice at each time point. **G–I** Inflammatory biomarkers MMP-9, CRP, and IL-6 were elevated at 4–8 h post-LBP dose and returned to baseline levels by 16–24 h. $N = 5$ mice at each time point. Mann–Whitney *U*-test and Kruskal–Wallis, Dunn's multiple comparisons. Bars represent the median ± interquartile range. $^{*}P < 0.05$, $^{**}P < 0.01$, $^{***}P < 0.001$, $^{****}P < 0.0001$.

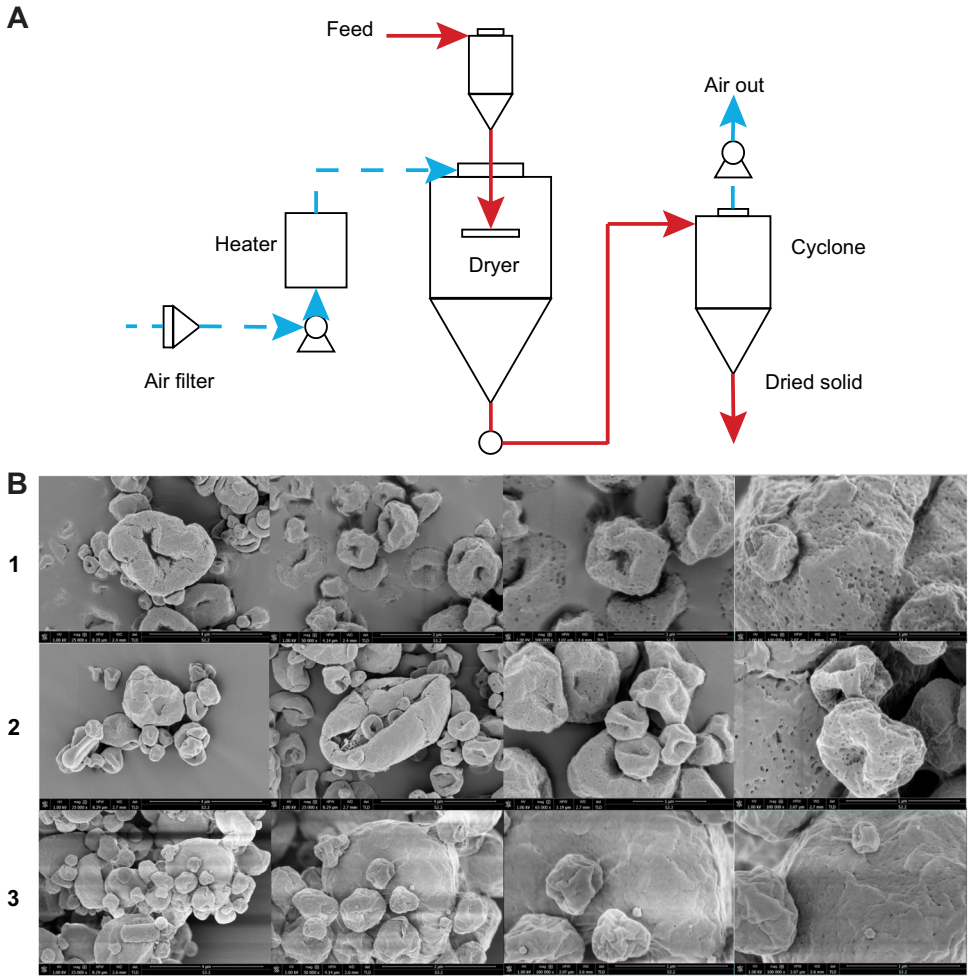

Fig. 5 | Spray drying produces small, flowable powder particles containing viable bacteria. A Schematic of spray drying process used to dry *Lactobacillus* strains into small, flowable powder particles. **B** Scanning electron microscope (SEM) images of three formulations of powder particles after drying. Images at 25,000, 50,000, and 100,000X magnification (left to right) were taken from one sample each.

UAB Regional Neonatal Intensive Care Unit. The protocol was approved by the IRB (IRB140926096) of the University of Alabama at Birmingham. A waiver of consent status was granted because the samples were obtained during routine clinical care and handled in a deidentified manner.

All animal protocols were submitted and approved by the IACUC of the University of Alabama at Birmingham (protocol 2002) consistent with the Public Health Service policy on Humane Care and Use of Laboratory Animals (Office of Laboratory Animal Welfare, 2002). Data was not collected disaggregated by sex due to lack of difference between male and female response in the models used.

Human cohort study for the role of Ac-PGP in severe BPD

Human tracheal aspirate collection. Tracheal aspirate samples were obtained from established severe BPD patients at 36 weeks post menstrual age as defined by physiologic definitions and gestational age-matched full-term controls[33]. Data was not disaggregated by sex. Samples were collected at the time of intubation prior to surgical procedures or anesthesia administration and served as controls. The samples were obtained after ensuring adequate oxygenation. The protocol for obtaining tracheal aspirates involved instilling 1 mL of sterile isotonic saline into the infant's endotracheal tube, manual bagging through the endotracheal tube for 3 breaths, and suctioning the fluid into a sterile mucus trap. The sample was centrifuged at 3000 × *g* for 10 min in order to separate the supernatant and cell pellet. Samples were frozen at −80 °C until further processing.

Analysis of Ac-PGP by electrospray ionization-liquid chromatography-tandem mass spectrometry. Acetylated PGP (Ac-PGP) was purchased from Bachem (Torrance, CA) and purified to neutrophil chemotactic activity. The Ac-PGP in tracheal aspirates was measured using an MDS Sciex API-4000 spectrometer (Applied Biosystems,

https://doi.org/10.1038/s41467-024-51169-0

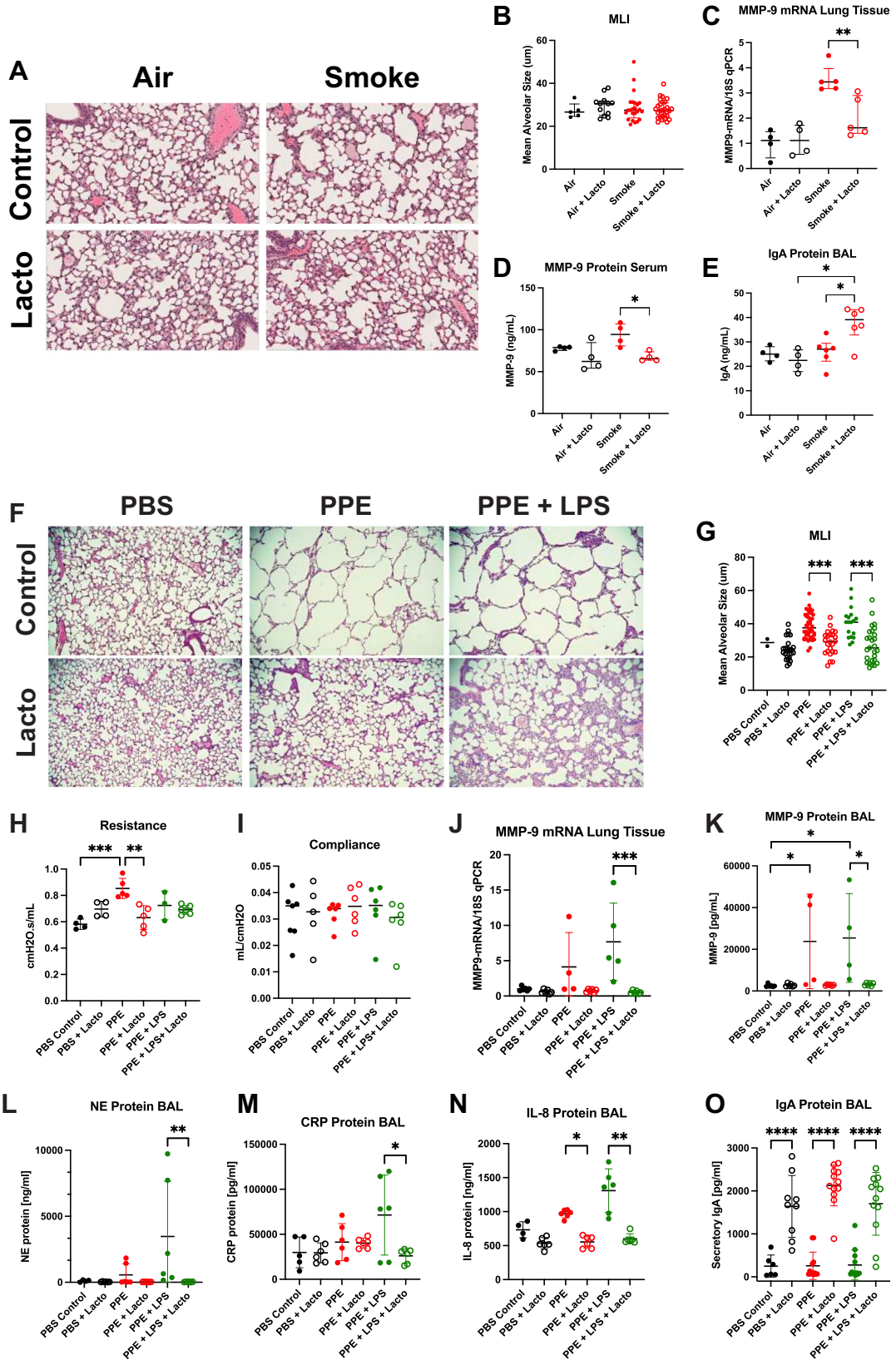

Carlsbad, CA) equipped with a Shimadzu HPLC (Columbia, MD). HPLC was performed using a 2.0_150-mm Jupiter 4 u Proteo column (Phenomenex, Torrance, CA) with Buffer A (0.1% HCOOH) and Buffer B (MeCN + 0.1% HCOOH). HPLC was initially performed with 95% Buffer A and 5% Buffer B from 0-0.5 minutes, then increased over 0.5–2.5 min to 0% Buffer A/100% Buffer B. Background was removed by flushing with 100% isopropanol/0.1% formic acid. Positive electrospray mass transitions were at 312-140 and 312-112 of Ac-PGP[10,34].

Endotoxin testing. Samples were tested using the Thermo Pierce Chromogenic Endotoxin Quantification Kit (A39552) according to the manufacturer's protocol.

Fig. 6 | *Lactobacillus*-based LBP improves biomarkers of inflammation and lung structure and function in murine models of COPD. Mice were exposed to cigarette smoke for 1 month and treated intratracheally with the *Lactobacillus* LBP (*Lacto*). **A** Lung histology image (H&E staining, 40x magnification) did not show significant worsening of alveolar structure upon 1 month of smoke exposure as measured by (**B**) and mean linear intercept (MLI). Measurements: Air $N = 5$, Air + Lacto $N = 11$, Smoke $N = 23$, Smoke + Lacto $N = 27$ samples. Mice exposed to smoke treated with *Lacto* showed improvements in (**C**) lung tissue MMP-9 expression (Air $N = 4$, Smoke $N = 5$ mice), **D** serum MMP-9 protein levels (Air $N = 4$, Smoke $N = 5$ mice), and **E** BAL IgA protein levels (Air $N = 4$, Smoke $N = 6$ mice). Mice were exposed to intratracheal porcine pancreatic elastase (PPE) and LPS, leading to significant alveolar hypoplasia and simplification. **F** Lung histology images (H&E staining, 4x magnification) showed that inhalation of the *Lacto* LBP concurrent with the injury period reduced tissue damage. **G** MLI improved upon treatment with *Lacto* LBP in PPE and PPE + LPS exposure groups. **H** Lung function worsened as measured by increased resistance upon exposure to PPE and improved upon treatment with *Lacto* LBP. **I** Lung function, as measured by compliance, showed no significant changes among groups. **J** MMP-9 expression in lung tissue increased upon PPE + LPS exposure and decreased upon treatment with *Lacto* LBP. **K** MMP-9 protein in the BAL increased upon PPE and PPE + LPS exposure and decreased upon treatment with *Lacto* LBP in PPE + LPS mice. **L** NE protein in the BAL decreased upon *Lacto* LBP treatment in PPE + LPS mice. **M** CRP protein in the BAL increased upon PPE + LPS exposure and decreased upon treatment with *Lacto* LBP. **N** IL-8 protein in the BAL decreased upon *Lacto* LBP treatment in PPE and PPE + LPS mice. **O** IgA protein in the BAL increased (improved) upon *Lacto* LBP treatment in control, PPE, and PPE + LPS mice. $N = 12$ mice (6 M/6 F). Kruskal–Wallis test, Dunn's multiple comparisons. Bars represent the median ± interquartile range. $^{*}P < 0.05$, $^{**}P < 0.01$, $^{***}P < 0.001$, $^{****}P < 0.0001$.

Analysis of MMP-9, MPO, and NE Protein by ELISA. MMP-9, MPO, and NE protein levels were measured using Human MMP-9, MPO, and NE DuoSet ELISAs (DY911; DY3174; DY9167-05, Biotechne), according to the manufacturer's protocol.

Lactobacillus LBP formulation

The *Lactobacillus* LBP material was developed in collaboration with Kindeva Drug Delivery (Woodbury, MN). The blend contains live *Lactobacillus* strains *Lactobacillus plantarum* BAA-793, *Lactobacillus acidophilus* 4356, and *Lactobacillus rhamnosus* 53103 spray-dried with trehalose, leucine, sodium citrate, and polysorbate as stabilizers in order to preserve viability of live cells while generating particle characteristics amenable for distal lung delivery. *Lactobacilli* strains are licensed from the American Type Culture Collection (ATCC).

Cell culture and treatment

Human bronchial epithelial cells (HBEC) (PCS-300-010, ATCC) were exposed to *E. coli*, hyperoxia, and/or treated with *Lactobacillus* strains or their components. Each experiment was performed in triplicate.

Hyperoxia model. Cells were exposed to 21% FiO_2 to represent normoxic conditions or 85% FiO_2 in a hyperoxia cell culture chamber to represent hyperoxic conditions. Cells were exposed to 1.0 µg/ml of *Escherichia coli* 055: B5 LPS (Millipore Sigma) or PBS as control.

***E. coli* + *Lactobacillus* model.** Six-well plates were inoculated with proteobacteria (*E. coli*), the *Lactobacillus* blend, or individual *Lactobacillus* strains *L. plantarum* (P), *L. acidophilus* (A), and *L. rhamnosus* (R). Strain blends were then compared at different ratios of P:A:R – 1:1:1, 3:1:1, and 1:3:1. P, A, and R activity in reducing MMP-9 was tested against four additional strains: *L. casei* (ATCC 393), *L. paracasei* (ATCC 25302), *L. reuteri* (ATCC 23272), and *L. fermentum* (ATCC 23271). *E. coli* (*E. coli* serotype K1) was grown on Luria Bertani (LB) broth containing 100 µg/ml of rifampin (Millipore Sigma). About 1×10^6 CFU of each bacteria strain P, A, and R was inoculated in 100 µl of antibiotic and serum-free media. Media without bacterial inoculation was used as a control. The supernatant (200 µl) was collected at 12 h from each well for each experiment.

***Lactobacillus* component testing.** Isolates and byproducts of the *Lactobacillus* strains P, A, and R were tested for MMP-9 reduction in the *E. coli* HBE model as previously described. L (+) and D (−) lactic acid were acquired commercially (L1750, Sigma). To collect bacterial cell culture supernatant, *Lactobacillus* strains were grown in an MRS medium for 16 h. Bacteria was then centrifuged, and the supernatant collected and passed through a 0.22-µm filter to eliminate any residual bacteria. Peptidoglycan was isolated from bacteria grown from overnight culture.

The bacterial culture was washed twice with saline and centrifuged at 15,000 × *g* for 10 min and 20,000 × *g* for 40 min. About 20 mL of 30% aqueous phenol pre-warmed to 90 °C was added to the suspension, the mixture was stirred for 20 min at 65–68 °C, cooled to 20 ± 2 °C, and was centrifuged three times for 10 min at 15,000 × *g*, removing supernatant each time. 30% aqueous phenol was added at 65–68 °C and distilled water to a total volume of 300 mL. About 3 mL of 100% acetic acid was added and stirred at 100 °C for 3 h. After cooling, the precipitate was placed on a magnetic stirrer for 10 min and centrifuged for 20 min at 20,000 × *g*. The precipitate was washed three times with water after each centrifugation. Dialysis was carried out at 21 ± 2 °C, removing dialysate three times per day and adding fresh 0.05 M sodium acetate solution (pH 5.8)[35]. Teichoic acid was isolated from bacteria grown from overnight culture at 4 °C on a magnetic stirrer. Centrifuged sediment was washed twice with 500 mL physiologic saline and the wet sediment was extracted three times with cold 10% TCA (100 mL each) and homogenized for 1 min. Precipitate was centrifuged after 12 h, washed with acetone, and washed with diethyl ether[36]. Purity was validated via mass spectrometry (Pacific Biolabs). S-layer was isolated from bacteria grown in overnight culture to the stationary phase (16 h), centrifuged at 2236×*g* for 10 min (4 °C), and washed twice with 25 mL cold PBS (Gibco). pH 7.4. 5 M LiCl (Fisher Scientific) was added, and cells were agitated for 15 min at 4 °C. Supernatant was harvested after centrifugation at 8994 × *g* for 10 min (4 °C) and transferred to a 6000–8000 kDa Spectra/Por molecular porous membrane (Spectrum Laboratories), then dialyzed against cold distilled water for 24 h (water changed every 2 h for the first 8 h). The dialyzed precipitate was harvested after 30 min centrifugation at 20,000 × *g* and was agitated for 15 min with 1 M LiCl at 4 °C. The suspension was centrifuged at 20,000 × *g* for 10 min and dialyzed again against cold distilled water for 24 h. Dialyzed precipitate was harvested after 30 min of centrifugation at 20,000 × *g*, and pellets were resuspended in 10% (w/v) SDS (Fisher)[37]. To isolate polysaccharides, cultured supernatant was collected, and 14% trichloroacetic acid was added to denature the protein material. The culture pellet was homogenized by the homogenizer (VELP Scientifica OV5 homogenizer) followed by centrifugation at 15,941×*g* for 20 min at 4 °C using the REMI centrifuge C24 plus. The supernatant was then added to cold absolute alcohol (1:3), incubated at 4 °C for 24 h, then centrifuged at 15,941×*g* for 20 min at 4 °C. Precipitate was dried for 24–48 h at 50 °C and concentration measured.

Antibiotic resistance and susceptibility panel. Each *Lactobacilli* strain in the LBP was evaluated for resistance and susceptibility against 51 FDA-approved antibiotics (Supplementary Tables 1, 2). Each strain, individually or as a blend, was plated in a lawn on agarose plates (2×10^8 CFU per plate) and incubated overnight at 37 °C with ETEST® strips for each antibiotic (Biomérieux) that indicated the minimum inhibitory concentration (MIC). If the strain was susceptible to the antibiotic, the strip inhibited the growth of the bacteria and indicated the lowest concentration of the antibiotic that would inhibit the visible growth of the bacteria. If the blend strain was resistant, the bacteria

https://doi.org/10.1038/s41467-024-51169-0

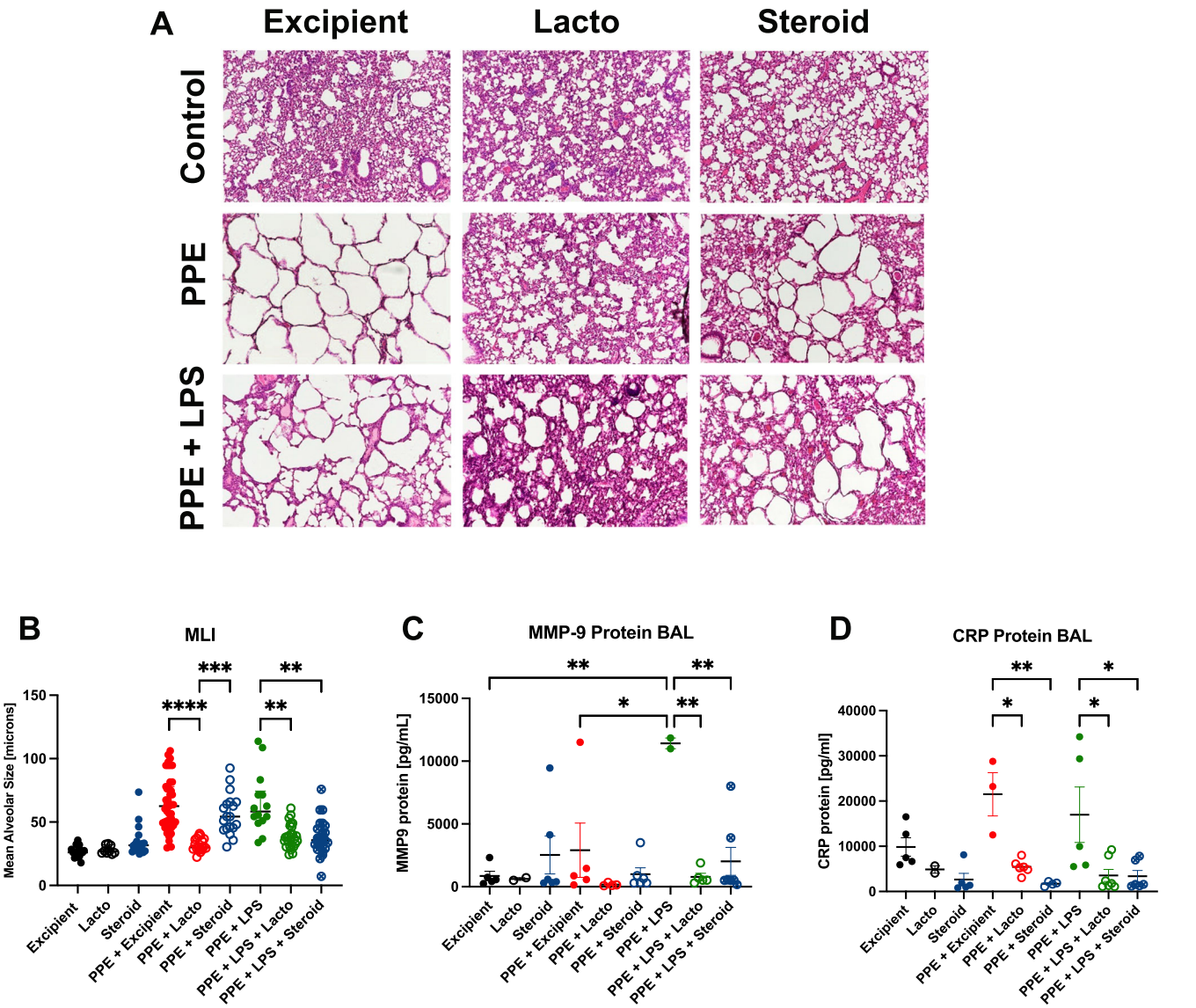

Fig. 7 | Mice were exposed to intratracheal PPE and LPS to establish emphysema and bacteria-driven inflammation. A Lung histology images (H&E staining, 4x magnification) show that *Lacto* LBP treatment after 2 weeks of injury was established, reduced inflammation, and improved tissue structure. Steroid treatment after injury decreases inflammation. **B** PPE and PPE + LPS exposure each increased mean alveolar size and *Lacto* LBP treatment significantly decreased (improved) it. The steroid fluticasone furoate (FF) also significantly reduced MLI but not as much as *Lacto* LBP in the PPE group. Measurements: Excipient $N = 16$, Lacto $N = 8$, Steroid N = 18, PPE + Excipient $N = 44$, PPE + Lacto $N = 18$, PPE + Steroid $N = 18$, PPE + LPS $N = 13$, PPE + LPS + Lacto $N = 24$, PPE + LPS + Steroid $N = 23$ samples. **C** *Lacto* LBP performed better than the steroid in reducing MMP-9 protein in BAL of mice exposed to PPE + LPS. **D** *Lacto* LBP performed as well as the steroid in reducing CRP protein in BAL of mice exposed to PPE and PPE + LPS. Excipient $N = 5$, Lacto $N = 2$, Steroid $N = 3$, PPE + Excipient $N = 3$, PPE + Lacto $N = 6$, PPE + Steroid $N = 4$, PPE + LPS $N = 5$, PPE + LPS + Lacto $N = 7$, PPE + LPS + Steroid $N = 6$ mice. Kruskal–Wallis test, Dunn's multiple comparisons. Bars represent the median ± interquartile range. $^{*}P < 0.05$, $^{**}P < 0.01$, $^{***}P < 0.001$, $^{****}P < 0.0001$.

grew uninhibited, and no inhibitory concentration was indicated on the strip.

Animal studies

C57BL/6 mice were obtained from The Jackson Laboratory (Bar Harbor, ME). Unless otherwise indicated, all experiments were performed with a minimum of 6–8 mice to detect a 25% difference with 80% power based on previous studies. Newborn pups were exposed to one of four BPD models: (1) Double-hit LPS+hyperoxia[16], (2) Ac-PGP gain-of-function, (3) Ac-PGP loss-of-function, (4) Double-hit LPS+hyperoxia with *Lactobacillus* LBP treatment. 10- to 12-week-old mice were inoculated with live *Lactobacillus* strains to measure bacteria survival and L(+) lactic acid production in the lungs. 10- to 12-week-old mice were exposed to 3 or 10 days of LPS IT and treated with IT L(+) lactic acid at concentrations of 0.125, 0.5, or 1.0 µg/g. 6- to 8-week-old mice were exposed to one of five COPD models treated with the *Lactobacillus* LBP: (1) Cigarette smoke[38], (2) Porcine pancreatic elastase (PPE) ± LPS[39], (3) LBP tolerated dose in PPE, (4) PPE ± LPS post-injury treatment, (5) Safety and biodistribution in PPE. See Supplement for details on approvals, exposure models, pulmonary function, and sample processing.

Animal studies

Double-hit murine BPD model. Newborn C57BL/6 mice were randomized to exposure groups with PBS control or incremental intranasal doses of *Escherichia coli* 055: B5 LPS (Millipore Sigma). Pups were dosed on postnatal day 3 (PN3) with 1 mg/kg, postnatal day 6 (PN6) with 2.5 mg/kg, postnatal day (PN9) with 5 mg/kg, and postnatal day 12

https://doi.org/10.1038/s41467-024-51169-0

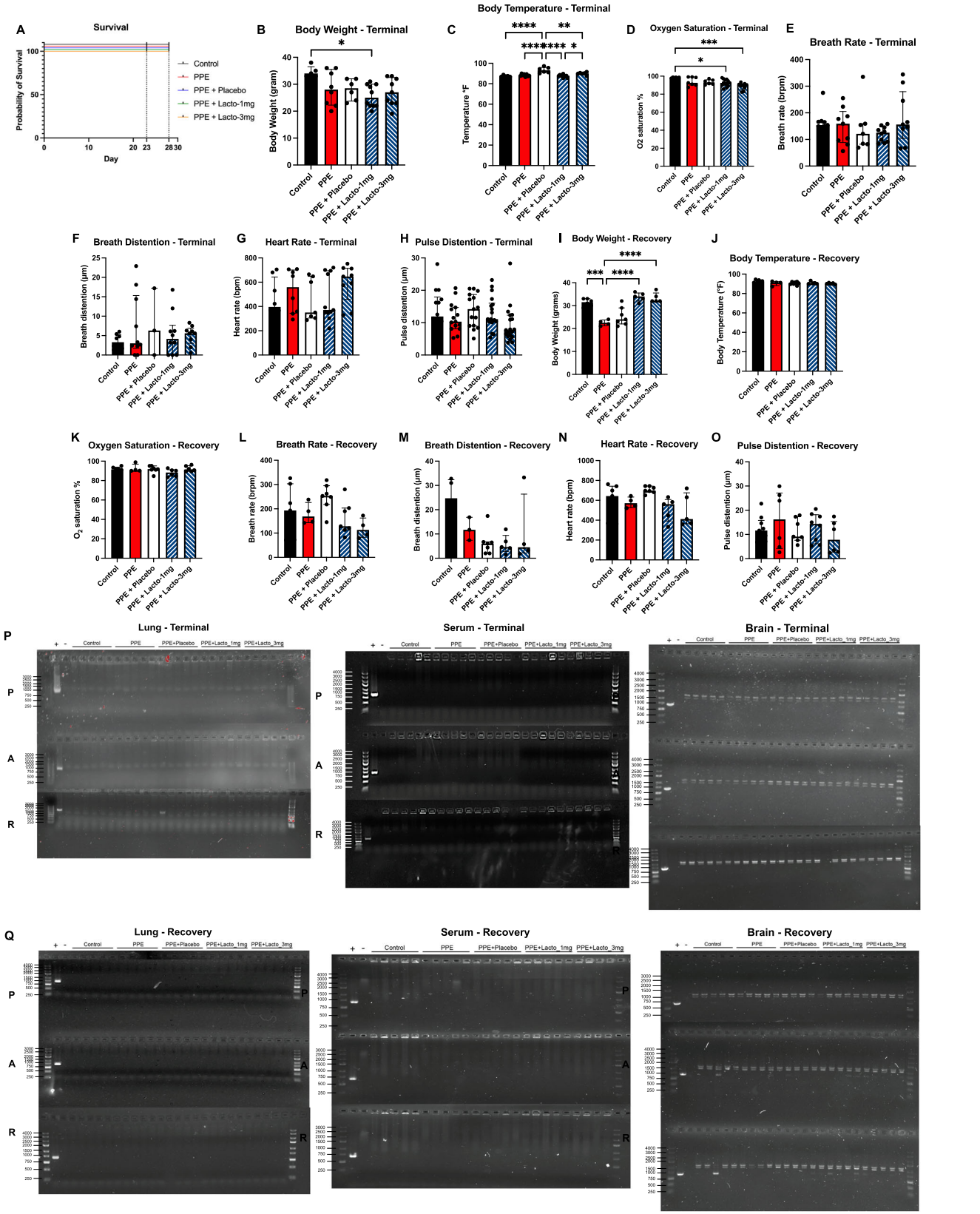

Fig. 8 | Inhaled *Lactobacillus*-based LBP shows favorable safety and biodistribution profile in the PPE mouse model. A 100% of the mice in the biodistribution study survived at 23 days (terminal sacrifice) and 28 days (recovery sacrifice). Survival curves offset for visibility. Body weight, temperature, oxygen saturation, breath rate, breath distension, heart rate, and pulse distension remained in normal ranges after 2 weeks of LBP dosing in **B**–**H** terminal sacrifice mice and **I**–**O** recovery sacrifice mice. **P** Representative gels from PCR on terminal sacrifice tissues lung, serum, and brain show no presence of LBP *Lactobacillus* strains. **Q** Representative gels from PCR on recovery sacrifice tissues lung, serum, and brain show no presence of LBP *Lactobacillus* strains. PBS and PPE control each $N = 10$; PPE + placebo, LBP 1 mg, LBP 3 mg each $N = 15$ mice. Kruskal–Wallis test, Dunn's multiple comparisons. Bars represent the median ± interquartile range. $^{*}P < 0.05$, $^{**}P < 0.01$, $^{***}P < 0.001$, $^{****}P < 0.0001$.

https://doi.org/10.1038/s41467-024-51169-0

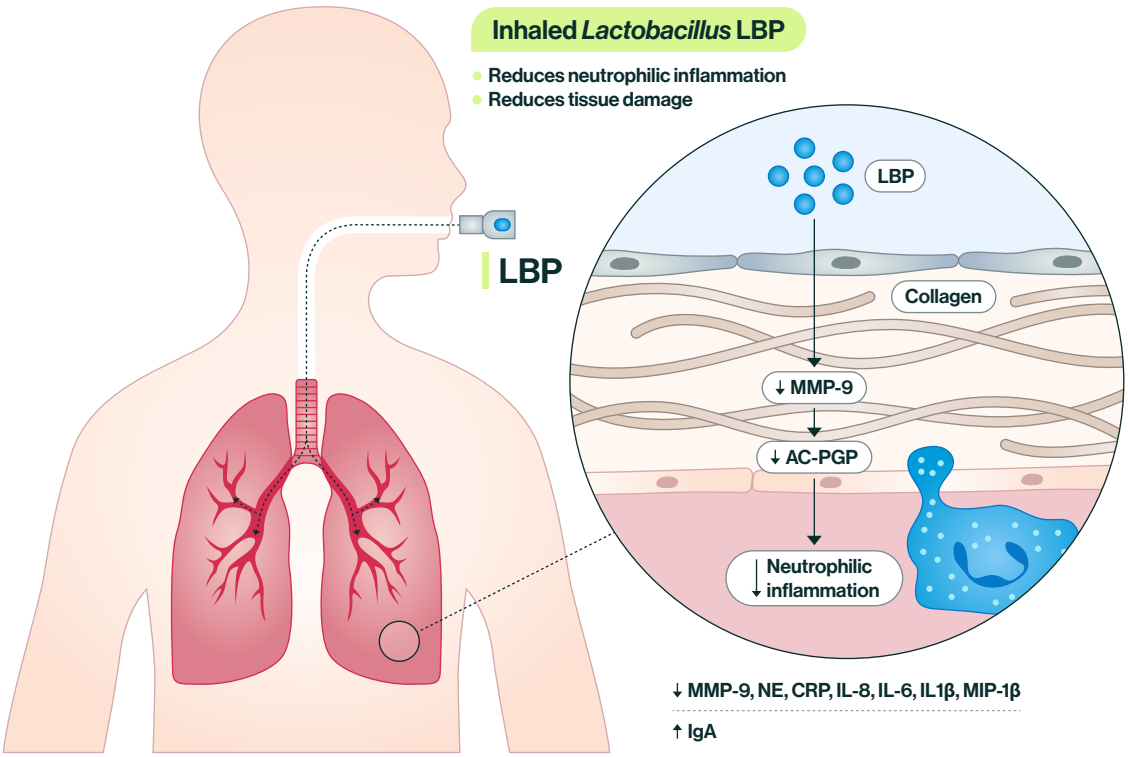

Fig. 9 | Schematic diagram of how the inhaled *Lactobacillus* LBP works. Particle engineering innovation facilitates the delivery of the *Lactobacillus* LBP directly into the lung to help reduce inflammation and restore lung tissue. Inhaled LBP releases anti-inflammatory metabolites that reduce MMP-9 and Ac-PGP expression and neutrophilic inflammation downstream. Other inflammatory biomarkers are reduced, and protective IgA is increased.

(PN12) with 7.5 mg/kg. Pups were also randomized to exposure to normoxia (21% FiO_2) or hyperoxia (85% FiO_2) from PN3-PN14. This represents the period of maximal alveolarization[40]. Surrogate dams were switched every 24 h from hyperoxia to normoxia to avoid oxygen toxicity. Daily animal maintenance was performed with exposure of the animals to room air for <10 min per day. A standard mouse pellet diet and water were provided ad libitum[40]. Pups were euthanized for tissue harvest on PN14. $N = 6–8$ mice per group.

Murine postnatal Ac-PGP gain-of-function model. Newborn C57BL/6 mice were randomized to treatment with normal saline control versus Ac-PGP (100 µg/25 µl saline). They received a total of four doses intranasally at PN3, PN6, PN9, and PN12. Pups were exposed to 21% FiO_2 or 85% FiO_2 from PN3-PN14 and were euthanized for tissue harvest at PN14. $N = 6–8$ mice per group.

Murine postnatal Ac-PGP loss of function model. Newborn C57BL/6 mice that were exposed to 85% FiO_2 and proteobacteria were randomized to treatment with arginine-threonine-arginine (RTR) versus normal saline at PN3, PN8, and PN13. The neutralizing Ac-PGP antagonist RTR, which functions to bind PGP both in vitro and in vivo, was synthesized by BACHEM (Torrance, CA) and administered intraperitoneally (50 µg/dose). Daily animal maintenance was performed as described above. $N = 6–8$ mice per group.

Lactobacillus LBP treatment in double-hit BPD model. Newborn C57BL/6 pups were exposed to 85% FiO_2 from PN3-PN14 in addition to *E. coli* (double-hit model as described above) and randomized to treatment with *Lactobacillus* LBP or treatment with PBS. Mice were inoculated intranasally with the LBP (1×10^8 total CFU) or PBS at PN3, PN6, PN9, and PN12 after 12 h of LPS administration. Daily animal maintenance was performed as described previously. Mice were euthanized for tissue harvest at PN14. $N = 6–8$ per group.

L (+) lactic acid treatment in LPS model. Three- to four-month-old female C57BL/6 mice were exposed to LPS IT (100 µg/mouse) to generate inflammation and tissue damage. Over the course of 3 or 10 days, mice were treated 3x with L (+) lactic acid at 0.5 µg/g or 1.0 µg/g and sacrificed on day 3. BAL, lungs, and serum were harvested. $N = 4$ per group.

In vivo strain survival and L (+) LA production. To determine whether administering live bacteria would be feasible from both dosing and viability perspectives, the lungs of 14 healthy 10–12-week-old female C57BL/6 mice were inoculated with 5×10^7 cells/mL of the live bacterial blend (P, A, R). Two mice were sacrificed at each time point: immediately after inoculation, and at 2, 4, 8, 12, 24, and 72 h after dosing ($N = 2$ each time point). Lung tissue and bronchoalveolar lavage (BAL) fluid were sampled and assessed for their bacterial signature. Lung tissue was homogenized in 1 mL PBS and plated on agarose plates in serial dilutions of 1 µL, 10 µL, and 100 µL. BAL was mixed with 500 µL PBS and plated on agarose plates in serial dilutions of 0.2, 2, and 20 µL. Plates were incubated for 16 h at 37 °C overnight and colonies were counted visually (ISO 7889). L (+) lactic acid levels in the lung tissue and BAL were quantified using a Lactate Colorimetric Assay according to the manufacturer's protocol (MAK064, Sigma). About 50 µL of the sample was loaded with Master Mix (46 µL lactate assay buffer, 2 µL lactate enzyme mix, 2 µL lactate probe) in a 96-well plate, incubated for 30 min, and absorbance measured at 570 nm.

In vivo LBP lung distribution visualization. Five C57BL6 mice were intratracheally inoculated (1×10^8 CFU) with live *Lactobacilli* stained for fluorescence: *Lactobacilli* blend – green, Mini67 (Sigma), nuclei – blue, Biotracker4000 (Sigma). Mice were sacrificed 3 h post-inoculation. Frozen lungs were sectioned at 12-µm thickness and visualized under a fluorescence microscope (Lionheart LX). Images were taken at 4x and 40x magnification. Scale bar at 1000 and 100 µm.

Cigarette smoke COPD model. Twenty 6 to 8-week-old female C57BL/6 mice were exposed to cigarette smoke ($N = 5$ mice per group) or air ($N = 4$ mice per group) and treated with a blend of P, A, and R strains or saline control. Mice who received smoke were exposed for 3 h a day Monday through Friday over a 1-month period. To smoke the mice, cigarette smoke from reference cigarettes RF2F (Tobacco and Health Research Institute, University of Kentucky) were diluted 1:1 and introduced into a chamber. Smoke was generated using the SCIREQ generator provided with the inExposure system. The nicotine concentration in the smoke using the above parameters was ~11 µg/l across all mice. The blend of strains was administered at a concentration of 1×10^8 CFU suspended in 50 µL of PBS after smoking. Mice were anesthetized and dosed IT with the *Lactobacillus* blend or 50 µL saline (control) every other day on Monday, Wednesday, and Friday. Mice were sacrificed after 4 weeks.

Porcine pancreatic elastase COPD model. Six to 8-week-old C57BL/6 mice were allocated into seven groups ($N = 6$ females, 6 males per group). The animals were administered 0.25 IU porcine pancreatic elastase (PPE) on Day 1 and Day 11 via oropharyngeal instillation to induce emphysema development over the course of the 3-week experiment. As injury, mice either received 50 µL PBS as a control, PPE, or a double-hit exposure of PPE and 1 h later, 100 µg of *E. coli*-derived lipopolysaccharide (LPS).

LBP powder tolerated dose test. In preparation for dosing mice with representative LBP drug product test material in a porcine pancreatic elastase (PPE) model of emphysema in COPD, several dose volumes of the LBP and dosing frequencies in mice with administration by Insufflator were tested. The Insufflator device is the representative equivalent of a dry powder inhaler (DPI) used in these mice. The active test material was a formulation containing spray-dried research-grade bacteria (2.4×10^{10} cells/mL) with trehalose, leucine, sodium citrate, and polysorbate as stabilizers. Placebo powder contained the same formula as the active without bacteria. 32 C57BL/6 mice (16 M, 16 F) were used in this week-long experiment (Supplementary Table 3). On Day 1, mice were Insufflated with 5 mg of LBP containing 1×10^8 CFU of live bacteria, 2.5 mg of LBP, followed by another 2.5 mg an hour later, 5 mg of placebo, or 50 µL PBS as a control. Mice continued to receive placebo or LBP dosages on Day 3 and Day 5. Five vital sign parameters were measured by MouseOximeter Plus (Starr Life Sciences) on Days 1, 3, and 5. Mice were connected to the MouseOx Plus for 20–30 min and multiple values were recorded for each mouse to minimize data variations in awake mice. Body weight and temperature were measured prior to vital signs. On Day 6, 24 h after the final dose administration, mice were sacrificed and lungs, serum, liver, and kidneys were collected for bacterial DNA PCR. Bacterial gDNA was extracted from all tissues (Zymo), and PCR was run to test for the presence of the three *Lactobacillus* strains using primers specific to each strain. The intensity of PCR products on agarose gels (1%) was quantified using ImageLab software.

Lactobacillus LBP co-treatment of PPE model mice. Beginning on Day 2, mice were treated with 1.5 mg of the *Lactobacillus* LBP containing 1×10^8 CFU live bacteria via Insufflator three times a week on Monday, Wednesday, and Friday for 3 weeks post-induction. The 1.5 mg absolute dose was chosen based on the results of a pilot dose tolerability test. Control groups with PBS, PPE, and PPE + LPS received 50 µL of PBS dosed every other day in lieu of the LBP. All animals were sacrificed 21 days after the first PPE induction.

Lactobacillus LBP post-injury treatment of PPE model mice. Following the design of the PPE model described above, mice began therapeutic treatment starting on Day 12, only after PPE injury had been established. Mice were treated 3 days per week using either PBS (control), LBP, or the inhaled corticosteroid fluticasone furoate (Sigma). Animals were sacrificed 21 days after the first PPE induction. $N = 5$ mice per group.

Safety and biodistribution in the PPE emphysema model. We conducted a respiratory safety and biodistribution study in PPE model mice. 70 mice total were exposed to PPE or PBS control ($N = 10$ per group) on Day 1 and Day 11 to establish an injury. Mice were dosed daily starting on Day 12 with nothing as a control against the placebo powder ($N = 15$), placebo powder ($N = 15$), a 1 mg dose of *Lacto* LBP (low dose, $N = 15$), or a 3 mg dose of *Lactobacillus* LBP (high dose, $N = 15$). Half the mice were euthanized on Day 23 for a terminal sacrifice ($N = 8$ per group) and the other half on Day 28 for a recovery sacrifice ($N = 7$ per group). Safety metrics and biodistribution samples were collected throughout, as described in Supplementary Table 4.

The MouseOx Plus machine (STARR Life Sciences Corp) was used to take the vital signs of each mouse individually. Vital signs included: body weight, temperature, heart rate, breath rate, pulse distension, breath distension, O_2 saturation, and ongoing cageside/clinical observations. Comprehensive tissue harvest was conducted to assess where, if at all, the *Lacto* LBP would distribute within the body. Bacterial gDNA was extracted from all tissues (Zymo), and PCR was run to test for the presence of the three *Lactobacillus* strains P, A, and R using primers specific to each strain. Intensity of PCR products on agarose gels (1%) were quantified using ImageLab software. BAL was plated at the terminal sac and recovery sac to assess if the *Lactobacillus* strains remained at the target tissue site.

Assessment of pulmonary function. At the end of hyperoxia or air exposure on PN14 (BPD model) or two days after the final LBP dose (COPD model), a subset of mice was anesthetized with isoflurane. The trachea was cannulated using a 24-gauge Angiocath and fixed with a 3-0 silk ligature. Pulmonary function was evaluated using a flexiVent apparatus (SCIREQ, Montreal, QC, Canada) that was equipped with a module 1 as described previously by ref. 41. This protocol was used for all in vivo experiments.

Right ventricular hypertrophy assessment. Right ventricular (RV) hypertrophy was assessed by measuring the whole heart weight, RV free wall weight, and an RV/(LV + S) ratio (Fulton index), where LV represents the left ventricle and S is the interventricular septum[42].

Animal harvesting. Mice were euthanized and randomly assigned for lung histology ($N = 6$), BAL ($N = 4$–6), or lung homogenates ($N = 6$). In order to harvest lung tissue for histology, the lungs were inflation-fixed via instillation of 0.3 mL of 10% formalin through the trachea. The chest was then opened, and the lungs were harvested and placed in 10% formalin. After ~24 h, the 10% formalin was exchanged for 100% isopropanol prior to being sent for processing. BAL was harvested by injecting 0.3 mL of PBS via the trachea at least twice. The sample was then flash-frozen in dry ice and stored at −80 °C for protein analysis. The left lower lobe of the lung was collected and processed to make whole lung homogenates[43]. For COPD model mice, serum was also harvested. These tissue harvest protocols were used in all in vivo experiments.

Analysis of alveolar morphometry. After harvest, the lung tissue was sliced into 5-micrometer sections, and they were stained with hematoxylin and eosin (H&E)[41,44,45]. Tissue imaging was performed with the software package MetaMorph version 6.2r4 (Universal Imaging) interfaced with a Nikon TE2000U microscope. The microscope was equipped with a QiCam Fast Cooled high-resolution CCD camera. Radial alveolar count (RAC) was used in the evaluation of alveolar lung development[41,45] in infant mice, and mean linear intercept (MLI) was

used to evaluate airspace enlargement in adult mice. To determine RAC, the number of septal junctions and branches were quantified using ImageJ software (version 1.54 f)[41]. MLI was determined using ImageJ software by analyzing fields of randomly placed, uniform-radius circles[46].

Ac-PGP mass spectrometry. The HPLC-MRM-MS analysis of samples was performed on the Shimadzu Prominence HPLC system with a refrigerated autosampler SIL-20A (Shimadzu Scientific Instruments, Inc. Columbia, MD) coupled with 4000 Triple quadrupole mass spectrometer (SCIEX, Framingham, MA, USA). Chromatography was performed using Jupiter 4 u Proteo column (80 Å, 150 × 2.1 mm Phenomenex, Torrance, CA). The mobile phase consisted of water with 0.1% v/v FA [A] and acetonitrile with 0.1% v/v FA [B] with a flow rate of 0.5 ml/min. The injection volume and total run time were 60 µl and 5 min, respectively. The column temperature was set at 40 °C. The operating parameters were: positive electrospray ionization mode with an electrospray voltage of 4000 V and an interface temperature of 600 °C. The curtain, GS1 and GS2 gas sources were set at 45, 50, and 50 PSI, respectively. Instrument parameters for the MRM transitions used were a Q1 mass of 312 and two Q3 masses (140 and 112). The LC-MS/MS system was controlled by Analyst software version 1.7.2.

MMP-9 qPCR. Total RNA from cells and homogenized lung tissue was extracted using TRIzol lysis reagent (15596026; Invitrogen, Waltham, MA, USA) and reverse transcribed using the SuperScript® III First-Strand Synthesis System for RT-PCR (18080-051, Invitrogen) per manufacturer's instructions. Quantitative real-time PCR (RT-PCR) was performed using primer-probes for human MMP-9 (Hs00957562_m1, Thermo Fisher) and mouse MMP-9 per manufacturer's instructions (Mm00442991_m1, Thermo Fisher). RT-PCR was performed on the MyiQ™ Single-Color Real-Time PCR detection System (Bio-Rad, Hercules, CA, USA) using SYBR Green PCR Master Mix per manufacturer's instructions (4309155; Applied Biosystems, Waltham, MA, USA). RT-PCR was performed using an initial 10 min denaturation period at 95 °C followed by 50 cycles of 15 s at 95 °C and 1 min annealing and extension at 60 °C. Expression levels of MMP-9 were normalized to 18 S RNA.

Analysis of MPO, MMP-9, CRP, IL-8 by ELISA. Using DuoSet ELISA (R&D Systems), natural and recombinant mouse MPO, MMP-9, CRP, and IL-8 were measured in BAL cell pellets and serum. BAL was centrifuged at 10,000 × *g* for 5 min, pellets were resuspended in 200 µl of PBS and further diluted by a factor of 10. About 100 µl of the sample was added per well. Samples were treated with detection antibody, followed by the streptavidin-HRP method. OD was measured at 450 nm in a microplate reader. Data were normalized to a standard curve.

Analysis of cytokines. Milliplex Mouse Cytokine Magnetic kits were custom-designed (Millipore Sigma) and used to measure an array of signaling proteins. The manufacturer instructions were followed. Median fluorescent intensity (MFI) data were used for calculating cytokine/chemokine concentrations in samples, using a five-parameter logistic method.

Transcriptomics

HBEC were exposed to the following noxious stimuli and/or treated with the LBP for 24 h.

1. PBS control
2. PBS + LBP
3. *Pseudomonas aeruginosa* (POA)
4. *Pseudomonas* + LBP
5. Cigarette smoke (S)
6. Cigarette smoke + LBP
7. Smoke + *Pseudomonas*
8. Smoke + *Pseudomonas* + LBP

RNA preparation: Cultured cells were lysed in RLT buffer (Qiagen) supplemented with 1% (w/w) 2-mercaptoethanol and RNA was isolated from cells with a RNeasy kit with Qiashredder cell disruption (Qiagen) and RNase-free DNase Set (Qiagen) on-column DNA digestion. RNA purity and concentration were assessed using an Agilent 2100 Bioanalyzer RNA Analysis chip (Eukaryote Total RNA Pico Series II) (Agilent Technologies).

RNAseq: Preparation of RNA library (mRNA library preparation (poly A enrichment) and transcriptome sequencing (NovaSeq PE150 (6 G raw data per sample) was conducted by Novogene Co., LTD, using the HiSeq 2500 platform (Illumina) with a pair-end 150-nucleotide read length. Raw sequencing data was mapped to the genome (GRCm39, mRNAGRCm39.109), raw and normalized counts (TPM) were determined, and differential gene expression was calculated using the CLC Genomic Workbench (GUI version, Qiagen). Genes with adjusted *p* value (q) <0.05 and log10 (Fold Change) >0.301 were considered as differentially expressed. Heatmaps and PC analyses/plots were generated using CLC Genomic Workbench. Differentially expressed genes were input for Ingenuity IPA (Qiagen) to identify significantly regulated networks and pathways.

Statistics and reproducibility

Data conforming to normal distribution were presented as mean ± standard error, while non-normal data were expressed as median ± interquartile range. For normally distributed data, two-way ANOVA was performed with multiple comparison testing using Tukey's method. Mann–Whitney *U*-test was performed on data with non-normal distribution for comparison between two groups or Kruskal–Wallis test for comparison between multiple groups. GraphPad Prism version 9.4 for Mac OS X (GraphPad Software; La Jolla, California) was used for all data analyses. $^{*}P < 0.05$ indicates statistical significance. No statistical method was used to predetermine the sample size. No data were excluded from the analyses. The Investigators were not blinded to allocation during experiments and outcome assessment.

Reporting summary

Further information on research design is available in the Nature Portfolio Reporting Summary linked to this article.

Data availability

The 16s data presented in this study (Fig. 1a) were previously published[12]. The RNAseq data generated in this study have been deposited in the Gene Expression Omnibus (GEO) under accession code GSE271605. Source data are provided with this paper.

References

1. Kalikkot Thekkeveedu, R., Guaman, M. C. & Shivanna, B. Bronchopulmonary dysplasia: a review of pathogenesis and pathophysiology. *Respir. Med.* **132**, 170–177 (2017).
2. Lohmann, P. et al. The airway microbiome of intubated premature infants: characteristics and changes that predict the development of bronchopulmonary dysplasia. *Pediatr. Res.* **76**, 294–301 (2014).
3. Bhandari, A. & Bhandari, V. Pathogenesis, pathology and pathophysiology of pulmonary sequelae of bronchopulmonary dysplasia in premature infants. *Front. Biosci.* **8**, e370–e380 (2003).
4. Glass, H. C. et al. Outcomes for extremely premature infants. *Anesth. Analg.* **120**, 1337–1351 (2015).
5. Stocks, J. & Sonnappa, S. Early life influences on the development of chronic obstructive pulmonary disease. *Ther. Adv. Respir. Dis.* **7**, 161–173 (2013).

6. Benjamin, J. T. et al. Neutrophilic inflammation during lung development disrupts elastin assembly and predisposes adult mice to COPD. *J. Clin. Invest.* **131**, e139481 (2021).
7. Richmond, B. W. et al. Airway bacteria drive a progressive COPD-like phenotype in mice with polymeric immunoglobulin receptor deficiency. *Nat. Commun.* **7**, 11240 (2016).
8. Richmond, B. W. et al. Bacterial-derived neutrophilic inflammation drives lung remodeling in a mouse model of chronic obstructive pulmonary disease. *Am. J. Respir. Cell Mol. Biol.* **58**, 736–744 (2018).
9. Genschmer, K. R. et al. Activated PMN exosomes: pathogenic entities causing matrix destruction and disease in the lung. *Cell* **176**, 113–126.e115 (2019).
10. Weathington, N. M. et al. A novel peptide CXCR ligand derived from extracellular matrix degradation during airway inflammation. *Nat. Med.* **12**, 317–323 (2006).
11. Huffnagle, G. B., Dickson, R. P. & Lukacs, N. W. The respiratory tract microbiome and lung inflammation: a two-way street. *Mucosal Immunol.* **10**, 299–306 (2017).
12. Lal, C. V. et al. The airway microbiome at birth. *Sci. Rep.* **6**, 31023 (2016).
13. Freeman, A. E. et al. Microbial induced redox imbalance in the neonatal lung is ameliorated by live biotherapeutics. *Am. J. Respir. Cell Mol. Biol.* **68**, 267–278 (2023).
14. Freeman, A. et al. MicroRNA 219-5p inhibits alveolarization by reducing platelet derived growth factor receptor-alpha. *Respir. Res.* **22**, 57 (2021).
15. Akthar, S. et al. Matrikines are key regulators in modulating the amplitude of lung inflammation in acute pulmonary infection. *Nat. Commun.* **6**, 8423 (2015).
16. Lal, C. V. et al. Exosomal microRNA predicts and protects against severe bronchopulmonary dysplasia in extremely premature infants. *JCI Insight* **3**, e93994 (2018).
17. Pammi, M. et al. Airway microbiome and development of bronchopulmonary dysplasia in preterm infants: a systematic review. *J. Pediatr.* **204**, 126–133.e122 (2019).
18. Sulaiman, I. et al. Lower airway dysbiosis augments lung inflammatory injury in mild-to-moderate COPD. *Am. J. Respir. Crit. Care Med.* **208**, 1101–1114 (2023).
19. Patel, D. F. et al. An extracellular matrix fragment drives epithelial remodeling and airway hyperresponsiveness. *Sci. Transl. Med.* **10**, eaaq0693 (2018).
20. Sharma, N. S. et al. The neutrophil chemoattractant peptide proline-glycine-proline is associated with acute respiratory distress syndrome. *Am. J. Physiol. Lung Cell Mol. Physiol.* **315**, L653–l661 (2018).
21. Barnes, P. J. The cytokine network in chronic obstructive pulmonary disease. *Am. J. Respir. Cell Mol. Biol.* **41**, 631–638 (2009).
22. Qiu, Y. et al. Biopsy neutrophilia, neutrophil chemokine and receptor gene expression in severe exacerbations of chronic obstructive pulmonary disease. *Am. J. Respir. Crit. Care Med.* **168**, 968–975 (2003).
23. Traves, S. L., Culpitt, S. V., Russell, R. E. K., Barnes, P. J. & Donnelly, L. E. Increased levels of the chemokines GROα and MCP-1 in sputum samples from patients with COPD. *Thorax* **57**, 590–595 (2002).
24. Gaggar, A. et al. A novel proteolytic cascade generates an extracellular matrix-derived chemoattractant in chronic neutrophilic inflammation. *J. Immunol.* **180**, 5662–5669 (2008).
25. Grumelli, S. et al. An immune basis for lung parenchymal destruction in chronic obstructive pulmonary disease and emphysema. *PLoS Med.* **1**, e8 (2004).
26. Saetta, M. et al. Increased expression of the chemokine receptor CXCR3 and its ligand CXCL10 in peripheral airways of smokers with chronic obstructive pulmonary disease. *Am. J. Respir. Crit. Care Med.* **165**, 1404–1409 (2002).
27. Calabrese, F. et al. IL-32, a novel proinflammatory cytokine in chronic obstructive pulmonary disease. *Am. J. Respir. Crit. Care Med.* **178**, 894–901 (2008).
28. Yang, K. et al. Lactate suppresses macrophage pro-inflammatory response to LPS stimulation by inhibition of YAP and NF-κB activation via GPR81-mediated signaling. *Front. Immunol.* **11**, 587913 (2020).
29. Ratter, J. M. et al. In vitro and in vivo effects of lactate on metabolism and cytokine production of human primary PBMCs and monocytes. *Front. Immunol.* **9**, 2564 (2018).
30. Maziak, W. et al. Exhaled nitric oxide in chronic obstructive pulmonary disease. *Am. J. Respir. Crit. Care Med.* **157**, 998–1002 (1998).
31. DiSantostefano, R. L. et al. Risk of pneumonia with inhaled corticosteroid versus long-acting bronchodilator regimens in chronic obstructive pulmonary disease: a new-user cohort study. *PLoS ONE* **9**, e97149 (2014).
32. Yang I. A. et al. Inhaled corticosteroids for stable chronic obstructive pulmonary disease. *Cochrane Database Syst. Rev.* **7** https://doi.org/10.1002/14651858.CD002991 (2012).
33. Walsh, M. C. et al. Impact of a physiologic definition on bronchopulmonary dysplasia rates. *Pediatrics* **114**, 1305–1311 (2004).
34. O'Reilly, P. et al. N-alpha-PGP and PGP, potential biomarkers and therapeutic targets for COPD. *Respir. Res.* **10**, 38 (2009).
35. Ziamko, V. & Okulich, V. Method of isolation of peptidoglycan as a basis for measuring murein-destroying activity of blood serum. *J. Microbiol. Exper.* **1**, https://doi.org/10.15406/jmen.2014.01.00025 (2014).
36. Carvalho, F., Pucciarelli, M. G., García-del Portillo, F., Cabanes, D. & Cossart, P. Extraction of cell wall-bound teichoic acids and surface proteins from Listeria monocytogenes. *Methods Mol. Biol.* **966**, 289–308 (2013).
37. Johnson, B., Selle, K., O'Flaherty, S., Goh, Y. J. & Klaenhammer, T. Identification of extracellular surface-layer associated proteins in *Lactobacillus acidophilus* NCFM. *Microbiology* **159**, 2269–2282 (2013).
38. Roda, M. A. et al. Proline-glycine-proline peptides are critical in the development of smoke-induced emphysema. *Am. J. Respir. Cell Mol. Biol.* **61**, 560–566 (2019).
39. Suki, B., Bartolák-Suki, E. & Rocco, P. R. M. Elastase-induced lung emphysema models in mice. *Methods Mol. Biol.* **1639**, 67–75 (2017).
40. Olave, N., Lal, C. V., Halloran, B., Bhandari, V. & Ambalavanan, N. Iloprost attenuates hyperoxia-mediated impairment of lung development in newborn mice. *Am. J. Physiol. Lung Cell Mol. Physiol.* **315**, L535–l544 (2018).
41. Nicola, T. et al. Hypoxia-induced inhibition of lung development is attenuated by the peroxisome proliferator-activated receptor-γ agonist rosiglitazone. *Am. J. Physiol. Lung Cell Mol. Physiol.* **301**, L125–L134 (2011).
42. Fulton, R. M., Hutchinson, E. C. & Jones, A. M. Ventricular weight in cardiac hypertrophy. *Br. Heart J.* **14**, 413–420 (1952).
43. Ambalavanan, N. et al. Transforming growth factor-beta signaling mediates hypoxia-induced pulmonary arterial remodeling and inhibition of alveolar development in newborn mouse lung. *Am. J. Physiol. Lung Cell Mol. Physiol.* **295**, L86–L95 (2008).
44. Dolma, K. et al. Effects of hyperoxia on alveolar and pulmonary vascular development in germ-free mice. *Am. J. Physiol. Lung Cell Mol. Physiol.* **318**, L421–l428 (2020).
45. James, M. L., Ross, A. C., Nicola, T., Steele, C. & Ambalavanan, N. VARA attenuates hyperoxia-induced impaired alveolar development and lung function in newborn mice. *Am. J. Physiol. Lung Cell Mol. Physiol.* **304**, L803–L812 (2013).
46. Crowley, G. et al. Quantitative lung morphology: semi-automated measurement of mean linear intercept. *BMC Pulmonary Med.* **19**, 206 (2019).

Acknowledgements
Research reported in this publication was supported by the National Heart, Lung, And Blood Institute of the National Institutes of Health under Award Number K08 HL141652 (CL), R35HL135710 (JB), R35HL166433 (JB), R01HL156275 (NA), and R44HL164156 (TN).

Author contributions
Conceptualization: T.N., N.W., N.A., A.G., and C.V.L. Experimentation: T.N., X.X., M.E., G.R., L.Q., and Y.Y. Analysis and interpretation: T.N., N.W., X.X., C.M., T.J., K.G., K.W., A.G., and C.L. Drafting and editing manuscript: T.N., N.W., N.A., A.G., and C.L. Funding acquisition and research supervision: T.N., K.W., N.A., J.B., A.G., and C.L. All authors have approved the final version of the manuscript as submitted.

Competing interests
Part of the research described in this manuscript is patented under "Inhaled Respiratory Probiotics for Lung Diseases of Infancy, Childhood and Adulthood" US 11,141,443 B2 held under the University of Alabama at Birmingham Research Foundation (CL, AG, NA are inventors). The remaining authors declare no competing interests.

Additional information
Supplementary information The online version contains supplementary material available at https://doi.org/10.1038/s41467-024-51169-0.

Correspondence and requests for materials should be addressed to Charitharth Vivek Lal.

Peer review information *Nature Communications* thanks Leopoldo Segal, and the other, anonymous, reviewer(s) for their contribution to the peer review of this work. A peer review file is available.